Received: 29 September 2023 | Accepted: 5 February 2024

DOI: 10.1111/jpy.13437

RESEARCH ARTICLE

Transcriptional responses to salinity-induced changes in cell wall morphology of the euryhaline diatom *Pleurosira laevis*

Shiho Kamakura[1] | **Gust Bilcke**[2,3,4] | **Shinya Sato**[5]

[1]Graduate School of Bioscience and Biotechnology, Fukui Prefectural University, Obama, Fukui, Japan

[2]VIB Center for Plant Systems Biology, Ghent, Belgium

[3]Department of Plant Biotechnology and Bioinformatics, Ghent University, Ghent, Belgium

[4]Protistology and Aquatic Ecology, Department of Biology, Ghent University, Ghent, Belgium

[5]Faculty of Marine Science and Technology, Fukui Prefectural University, Obama, Fukui, Japan

Correspondence
Shinya Sato, Fukui Prefectural University, 1-1 Gakuen-cho, Obama, Fukui 917-0003, Japan.
Email: ssato@fpu.ac.jp

Present address
Shiho Kamakura, KYOUSEI Science Center for Life and Nature, Nara Women's University, Nara, Japan.

Funding information
Japan Society for the Promotion of Science, Grant/Award Number: 20K06726 and 21A402

Editor: N. Poulsen

Abstract

Diatoms are unicellular algae with morphologically diverse silica cell walls, which are called frustules. The mechanism of frustule morphogenesis has attracted attention in biology and nanomaterials engineering. However, the genetic regulation of the morphology remains unclear. We therefore used transcriptome sequencing to search for genes involved in frustule morphology in the centric diatom *Pleurosira laevis*, which exhibits morphological plasticity between flat and domed valve faces in salinity 2 and 7, respectively. We observed differential expression of transposable elements (TEs) and transporters, likely due to osmotic response. Up-regulation of mechanosensitive ion channels and down-regulation of Ca^{2+}-ATPases in cells with flat valves suggested that cytosolic Ca^{2+} levels were changed between the morphologies. Calcium signaling could be a mechanism for detecting osmotic pressure changes and triggering morphological shifts. We also observed an up-regulation of ARPC1 and annexin, involved in the regulation of actin filament dynamics known to affect frustule morphology, as well as the up-regulation of genes encoding frustule-related proteins such as BacSETs and frustulin. Taken together, we propose a model in which salinity-induced morphogenetic changes are driven by upstream responses, such as the regulation of cytosolic Ca^{2+} levels, and downstream responses, such as Ca^{2+}-dependent regulation of actin dynamics and frustule-related proteins. This study highlights the sensitivity of euryhaline diatoms to environmental salinity and the role of active cellular processes in controlling gross valve morphology under different osmotic pressures.

KEYWORDS
cytoskeletal element, morphological plasticity, osmotic pressure, polymorphism, RNA-Seq, transporter, valve morphogenesis

Abbreviations: ARP, actin-related protein; CPM, counts per million; DEG, differentially expressed gene; DMSP, dimethylsulfoniopropionate; FC, fold change; FDR, false discovery rate; GO, Gene Ontology; SDV, silica deposition vesicle; SLC, solute carrier; TCDB, Transporter Classification Database; TE, transposable element.

INTRODUCTION

Diatoms are microalgae distributed in a wide range of aquatic and terrestrial environments throughout the world. The major feature of diatoms is that they have cell walls called frustules, composed of silica. Frustules consist of two valves separated by girdle elements and display diverse and intricate morphologies, including micrometer-scale exteriors and fine structures, such as pores and their occlusions, in the order of tens to hundreds of nanometers. The morphogenesis of frustules occurs in silica deposition vesicles (SDVs), which are compartments separated by lipid bilayer membranes located immediately beneath the plasma membrane of dividing daughter cells (Kröger & Poulsen, 2008; Pickett-Heaps et al., 1990). The morphology of the SDV, including the frustule that forms inside it, is regulated by cytoskeletal elements in the vicinity of the SDV (Pickett-Heaps et al., 1990; Tesson & Hildebrand, 2010a). The cytoskeletal elements define the position of the outer edges and structures of the valve (Tesson & Hildebrand, 2010a, 2010b) and influence the pattern of the pores (Pickett-Heaps et al., 1990). Furthermore, some proteins involved in silica mineralization and frustule formation have been identified (De Sanctis et al., 2016; Görlich et al., 2019; Heintze et al., 2022; Kröger et al., 2002; Nemoto et al., 2020; Scheffel et al., 2011; Tesson et al., 2017; Trofimov et al., 2019). Since the species-specific morphology and structure of diatoms may be tied to their function and contribute to the fitness of individuals (Finkel & Kotrc, 2010), the cellular and genetic pathways underlying the species-specific frustule morphologies have been a fascinating biological inquiry. In addition, the morphogenesis of the frustule is of interest due to its potential application in the massively parallel production of silica nanomaterials by self-assembly (Kröger & Poulsen, 2008).

Schmid (1987) proposed that the three-dimensional morphology of the valves could be controlled by the pressure on the daughter plasma membrane at the cleavage furrow, exerted by turgor pressure. According to Schmid, a flat valve face is formed when the tension of the daughter membrane is high due to turgor pressure, and the force exerted on the forming valve from within the cell is greater than that on the girdle region. Conversely, the opposite occurs in some marine diatoms: When the force on the girdle region is greater than that on the valve face, the daughter membrane tension is low, and the cell sometimes plasmolyzes, resulting in a valve face with ridges and grooves (see also Mann, 1984). The association between osmotic pressure and valve morphology has been supported by studies in *Skeletonema* species (Balzano et al., 2011; Paasche et al., 1975) and *Pleurosira laevis* (Kamakura et al., 2022). Kamakura et al. (2022) showed that *P. laevis* changed its valve morphology in response to the environmental osmotic pressure. *Pleurosira laevis* formed a flat valve face at salinity 2, whereas it formed a dome-shaped valve face at salinity 7. This response was conserved among strains collected from different environments. The morphological plasticity seen in *P. laevis* is a rare characteristic within diatoms, and it makes this species ideal for examining the underlying molecular basis of three-dimensional morphogenesis. In the present study, we generated a de novo transcriptome of *P. laevis* and characterized the gene expression of two different strains, each cultivated in salinities of 2 and 7. Differential expression analysis allowed us to explore the genes that were involved in the regulation of frustule morphology.

MATERIALS AND METHODS

Culture

The strains HA-01 and HA-02 of *Pleurosira laevis*, obtained from freshwater (Kamakura et al., 2022), were cultivated using WC medium (Guillard & Lorenzen, 1972) modified to salinity 2 and 7 by adding a salt stock described by Nakov et al. (2020). The media were adjusted to pH 8 by dropwise addition of 1 M HCl and then sterilized through a membrane filter (pore size 0.2 μm, mixed cellulose ester, Advantec, Tokyo, Japan). Cells were cultivated at salinity 2 or 7, at 18°C, under a 12:12 light:dark condition of cold white light with an intensity of ca. 20 μmol photons · m^{-2} · s^{-1}, in culture flasks (Nunc EasYFlask Cell Culture Flasks, Thermo Fisher Scientific, Massachusetts, USA).

RNA extraction and sequencing

Cells that had been cultivated at a salinity of 2 or 7 for more than 1 month were collected on membrane filters (pore size 8 μm, polycarbonate, Advantec), and total RNA was extracted by the cetyltrimethylammonium bromide method (Imaizumi et al., 2000). The experiment was performed in triplicate for the two strains under the two salinity conditions, resulting in 12 samples. The concentration of RNA was measured using a Qubit 4 Fluorometer (Thermo Fisher Scientific). Libraries of cDNA were prepared using TruSeq Stranded mRNA Library Prep Kit (Illumina, California, USA). Sequencing on a NovaSeq 6000 system (Illumina, paired-end, read length 100 bp) yielded 5.7–7.2 Gb of reads from each sample. The raw fastq files are available in the Sequence Read Archive (NCBI) under project number PRJNA1073709 (https://www.ncbi.nlm.nih.gov/bioproject/PRJNA1073709).

De novo transcriptome assembly

Pre-processing by fastp ver. 0.20.0 (Chen et al., 2018) was performed with default parameters to remove sequencing adapters and error-prone sequences from data sets. Next, de novo assembly was carried out by Trinity ver. 2.14.0 (Grabherr et al., 2011) with default parameters combining a total of 12 pre-processed paired-end reads of strains HA-01 and HA-02. Sequence redundancy was eliminated by clustering sequences with >95% homology using CD-HIT ver. 4.8.1 (Fu et al., 2012), and then, sequences shorter than 500 bp were removed using seqkit ver. 0.13.2 (Shen et al., 2016). To determine how complete this de novo transcriptome was, we performed a core gene family completeness test using TRAPID 2.0 (Bucchini et al., 2021), specifying the "Bacillariophyta" (diatom) clade and choosing a conservation threshold of 0.8.

To address potential mapping issues to the hybrid transcriptome because of sequence divergence between strains, we also independently assembled the RNA-Seq reads of each of the two strains using Trinity, generating distinct transcriptomes. Subsequently, we compared the mapping rates through RSEM ver. 1.3.3 (Li & Dewey, 2011) for these separate transcriptomes with those of the hybrid transcriptome and determined no relevant differences (mean alignment rate: hybrid 86.6%, HA-01 87.8%, HA-02 87.0%). Additionally, we identified key genes (the candidate BacSET, BacSET-like, frustulin, annexin, ARPC1, MS ion channels, and Ca^{2+}-ATPases observed in the hybrid assembly, see Results and Discussion) in the strain-specific transcriptome assemblies through blastn (BLAST+ ver. 2.9.0, Zhang et al., 2000). The best hit sequences with an E-value < 1E-4 were considered homologs of the key genes. The response in gene expression for these key genes in the strain-specific assemblies was visually verified to confirm robustness of the results obtained from the hybrid transcriptome (Figure S1 in the Supporting Information). The hybrid assembly and read count table used are available as Appendices S1 and S2 in the Supporting Information, and the strain-specific assemblies and read count tables are available upon request to the corresponding author.

The assembled contigs were submitted to the metagenomic classifier Kaiju webserver (Menzel et al., 2016, https://kaiju.binf.ku.dk/server) against the NCBI reference protein database (nr+euk, database date 2021-02-24) with default parameters (Greedy mode, minimum match length 11, minimum match score 75, allowed mismatches 5, max E-value 0.01). Sequences classified as bacteria, archaea, and opisthokonta were identified as potentially derived from contaminants. We flagged 5861 contaminant sequences, and they were eventually removed from the list of differentially expressed genes (DEGs) after read mapping and differential expression analysis, described below.

Read count and differential expression analysis

Hereafter, a *Pleurosira laevis* "gene" refers to a gene as defined by the Trinity assembler (".gX"). Read counts were performed using RSEM with the assembled sequences as reference through the Trinity script align_and_estimate_abundance.pl, with default parameters. The counts of different isoforms were summed for each gene, then TMM (trimmed mean of M value) was normalized using the R package edgeR ver. 3.28.0 (Robinson et al., 2010; Robinson & Oshlack, 2010). A negative binomial generalized linear model (GLM) test was performed to detect DEGs between salinity 2 and 7. Genes with a false discovery rate (FDR) < 0.05 and fold change (FC) > 2 between the salinity conditions were considered differentially expressed. The differential expression analysis was performed independently for HA-01 and HA-02. Then, the intersection of DEGs shared between HA-01 and HA-02 was determined by the web application "Calculate and draw custom Venn diagrams" provided by Ghent University (https://bioinformatics.psb.ugent.be/webtools/Venn/). We selected genes that (1) shared differential expression between both strains and (2) were responsive in the same direction (up-/down-regulated) in both strains, and we regarded them as genes with a conserved response for functional interpretation.

To visualize the variation between samples we made a multidimensional scaling (MDS) plot with the plotMDS function of the R package limma ver. 3.46.0 (Ritchie et al., 2015) using TMM-normalized read counts. The pairwise distances between the samples were determined based on the log2 fold changes in the 500 most variable genes (except for the contaminant sequences) between the samples. We also made a heatmap based on the Poisson distances between samples calculated using TMM-normalized read counts by the PoissonDistance function in the R package PoiClaClu ver. 1.0.2.1 (Witten, 2011).

Functional annotation

TransDecoder ver. 5.5.0 (https://transdecoder.github.io/) was used to predict protein-coding regions within transcripts via Pfam searches (database ver. 33.1, Mistry et al., 2021) to identify protein domains with the --single_best_only option. The predicted regions were converted to protein sequences. The longest predicted protein sequence for each gene was extracted via seqkit and used for functional annotation. We performed InterProScan (Jones et al., 2014) on Blast2GO ver. 6.0.3 (Conesa et al., 2005; Götz et al., 2008) against InterPro protein signature databases (Paysan-Lafosse et al., 2023), including Pfam, CATH-Gene3D, SUPERFAMILY, MobiDB-lite,

COILS, CDD, HAMAP, PANTHER, TIGRFAMs, PIRSF, PROSITE profiles, and SMART. As a result, 5280 genes were each assigned one or more InterPro accessions. We then obtained KEGG pathway annotations via the KofamKOALA web server ver. 2022-08-01 (KEGG release 103.0, Aramaki et al., 2020, https://www.genome.jp/tools/kofamkoala/) with an E-value threshold of 0.01 (default).

The DEGs were additionally annotated with Gene Ontology (GO) mapping based on a blastp search against NCBI protein database (nr) on Blast2GO with an E-value threshold of 1E-3. Up to 10 blast hits were used for GO mapping for each gene. Differentially expressed genes encoding putative transporters were further subjected to a blastp search against the Transporter Classification Database (TCDB, Saier et al., 2021, https://www.tcdb.org/) and assigned TC numbers. The DEGs encoding putative TEs were additionally annotated based on the transcript nucleotide sequences by blastx with E-value threshold of 0.1 against the retrotransposon protein domain database CORES, downloaded from the Gypsy Database (GyDB 2.0, Llorens et al., 2011, https://gydb.org/).

To investigate the response of cell wall-related genes to salinity-induced morphological changes, we identified *Pleurosira laevis* orthologs of marker genes for cell wall-related processes. First, the longest isoform (transcript) of each *P. laevis* gene was assigned to a PLAZA Diatoms ver. 1.0 gene family using TRAPID 2.0. Next, we screened for DEGs belonging to a list of previously annotated cell wall marker gene families, which includes among others the frustulins, BacSETs, silicanins, SiMATs, and p150 proteins (Bilcke et al., 2021). To ensure the correct identification of these candidate *P. laevis* cell wall proteins, blastp searches were performed back against the PLAZA Diatom protein database (E-value 1E-5; Osuna-Cruz et al., 2020). We next focused on cytoskeletal elements—actin, actin-related proteins, and tubulin—which also affect the morphogenesis of the diatom frustule (Tesson & Hildebrand, 2010a, 2010b). To search for tubulins and actin-related genes in our data set, we obtained the protein sequences of the model diatoms *Thalassiosira pseudonana*, *Phaeodactylum tricornutum*, *Pseudo-nitzschia multiseries*, and *Fragilariopsis cylindrus* from the Joint Genome Institute (JGI) PhycoCosm (Grigoriev et al., 2021, https://phycocosm.jgi.doe.gov) and ran OrthoFinder ver. 2.5.2 (Emms & Kelly, 2019) with default parameters along with our protein sequences of *P. laevis* genes used for the functional annotation query. We then picked up the genes that formed orthogroups with actin-related proteins identified by Aumeier (2014) and Aumeier et al. (2015) and tubulins identified by Khabudaev et al. (2022; Table S1 in the Supporting Information).

Markers for different stages of the cell cycle were retrieved from Bilcke et al. (2021). For each *Seminavis robusta* marker gene, all *Pleurosira laevis* genes belonging to the same PLAZA Diatoms homologous gene family were selected. Subsequently, a protein similarity search of the *P. laevis* candidate proteins against the *S. robusta* proteome was performed with Diamond blastp ver. 2.0.14, and only those *P. laevis* candidate genes for which the best blast hit was a known *S. robusta* cell cycle marker were retained.

Enrichment analysis

InterPro accessions significantly enriched in DEGs shared in both strains were detected via Fisher's exact test with FDR < 0.05, using FatiGO (Al-Shahrour et al., 2007). The accessions assigned to all genes by InterProScan were used as background of the analysis. The gene ratios were calculated by dividing the count of each InterPro accession assigned to the shared up- or down-regulated genes by the total count of each accession assigned to all genes.

Phylogenetic analysis

To understand the function or intracellular localization of Ca^{2+}-ATPases, we built a phylogenetic tree using all the protein sequences of *Pleurosira laevis* genes that matched any Ca^{2+}-ATPases from TCDB (TC: 3.A.3.2) in a blastp search with an E-value threshold of 1E-3. A phylogenetic analysis was performed by aligning protein sequences with MAFFT ver. 7.453 (Katoh et al., 2002), automatic trimming with TrimAL ver. 1.4.1 (Capella-Gutiérrez et al., 2009; gap threshold of 0.5), and tree construction with IQ-tree ver. 2.1.3 (Nguyen et al., 2015; automatic model selection, 1000 ultrafast bootstrap repeats).

For phylogenetic analysis of HCO_3^- transporters and TEs, multiple sequence alignments were performed using MAFFT ver. 7.480 with the --auto option, and sites with more than 30% gaps were removed using trimAl. Maximum likelihood trees were constructed using RAxML version 8.2.12 (Stamatakis, 2014) with the PROTGAMMAAUTO substitution model and 100 bootstrap replicates and were visualized using MEGA version 7.0.26 (Kumar et al., 2016). The sequence of *Odontella aurita* used in the analysis of the HCO_3^- transporter was obtained through the following process: The whole transcriptome of *O. aurita* from the MMETSP database (NCBI accession SRR1294405, Keeling et al., 2014) was pre-processed by fastp, de novo assembled by Trinity, clustered with 90% identity by CD-HIT, and then converted to protein sequence by TransDecoder. Orthologs from the whole transcriptome of *O. aurita* were searched for by running Orthofinder along with the protein sequences of HCO_3^- transporters from mammals, plants, fungi, and

eukaryotic algae listed in "data set S1" in Nakajima et al. (2013). Phylogenetic analysis of HCO_3^- transporters was conducted using the protein sequences of HCO_3^- transporters from *P. laevis*, *O. aurita*, and organisms listed in data set S1 in Nakajima et al. (2013), as well as sequences of other diatoms that hit by blastp with the sequences of HCO_3^- transporter of *P. laevis* in the annotation process. For TE analysis, we used the protein sequences of CoDi (Ty1/Copia-like elements from diatoms) and GyDi (Ty3/Gypsy from diatoms) provided by Maumus et al. (2009) and the sequences of selected retrotransposons from *P. laevis*, as well as retrotransposons from model organisms (Ty1 and Ty3 from *Saccharomyces cerevisiae*, Copia from *Drosophila melanogaster*, and Tnt1 from *Nicotiana tabacum*). In instances where open reading frames (ORFs) derived from a single TE were divided into group-specific antigen (gag) and polymerase (pol), they were concatenated in the sequence gag-pol for further phylogenetic analysis. (Note that the ORFs of gag and pol of the model diatoms used in this study do not overlap.)

We performed a reconstruction of the ancestral habitat (marine or freshwater-tolerant) based on SSU rDNA gene phylogeny. The SSU rDNA gene sequences from *Pleurosira* and *Odontella*, and other species phylogenetically close to *P. laevis* (Li et al., 2018) were aligned through ClustalW (Thompson et al., 1994) and manually trimmed to 1563 bp on BioEdit ver. 7.2.5 (Hall, 1999). Maximum likelihood trees were constructed using RAxML with the GTRGAMMA substitution model and 1000 bootstrap replicates. The reconstruction of the ancestral habitat was performed under the Markov k-state one-parameter model using Mesquite ver. 3.70 (Maddison & Maddison, 2021). The natural growth environments of the selected diatoms were determined based on information from collection sites provided by the Roscoff Culture Collection (http://roscoff-culture-collection.org/), as well as from Schmidt (1875), Ashworth et al. (2013), Li et al. (2018), Kamakura et al. (2022), and appendix 1 in Mann (1999).

RESULTS AND DISCUSSION

Transcriptome assembly and differential expression analysis

De novo transcriptome assembly of the *Pleurosira laevis* RNA-Seq reads resulted in a set of 192,661 transcripts (117,658 genes). To remove redundancy and low-quality transcripts, the sequences were clustered at 95% identity via CD-HIT, and sequences shorter than 500 bp were removed. This resulted in a transcriptome of 72,859 transcripts belonging to 50,070 genes, with quality illustrated by a diatom gene family completeness score of 0.908. Protein-coding regions in the transcripts were predicted by TransDecoder, yielding protein sequences for a total of 60,068 transcripts (33,994 partial sequences and 26,074 complete sequences) belonging to 38,275 genes.

We performed read mapping and expression quantification using this assembly as a reference and observed that the number of genes detected to be expressed in HA-01 was greater than that in HA-02 (Figure S2a in the Supporting Information). Out of the 23,830 genes expressed with counts per million (CPM) > 1 in the de novo transcriptome, 18,024 genes were expressed in both strains, while over 5000 genes were expressed in only one of the strains (Figure S2b). Next, DEGs were detected with FDR < 0.05 and fold change > 2. We selected the higher salinity (salinity 7) as the baseline for the differential expression analysis, based on the fact that the ancestor of *Pleurosira laevis* is marine, and it likely recently colonized freshwater and brackish water (see Bicarbonate transport section in Transmembrane transport). The number of genes up-regulated in salinity 2 (flat-shaped) was 2099 in HA-01 and 2580 in HA-02, while the number of genes down-regulated in salinity 2 compared with salinity 7 (dome-shaped) was 1978 in HA-01 and 2577 in HA-02 (Figure 1a,b). We focused on the functions of up- or down-regulated genes that were shared between the strains HA-01 and HA-02, specifically the genes included in [i] and [ii] in the Venn diagram in Figure 1b, to understand the core response to salinity behind the morphological plasticity in *P. laevis*.

Intraspecific variation in responses to salinity in *Pleurosira laevis*

An MDS plot (Figure 2a) and a Poisson-distance heatmap (Figure 2b) showed that the samples clustered predominantly by strain. The different responses to salinity between the strains might be due to local adaptations derived from differences in natural habitats: HA-01 was collected from a purely freshwater environment, whereas HA-02 was collected from an environment with a sporadic inflow of seawater (Kamakura et al., 2022). Recent studies have shown that even within a single diatom species, different strains exhibit various patterns of gene expression in response to the environmental factors (temperature, Pargana et al., 2019; salinity, Nakov et al., 2020; Pinseel et al., 2022). Conversely, the Poisson distance heatmap also showed a correlation in response to the same salinity treatment among different strains, suggesting a core-conserved response to salinity. Despite there being more unshared DEGs than shared ones between HA-01 and HA-02 in both the up and down-regulated gene sets (Figure 1b),

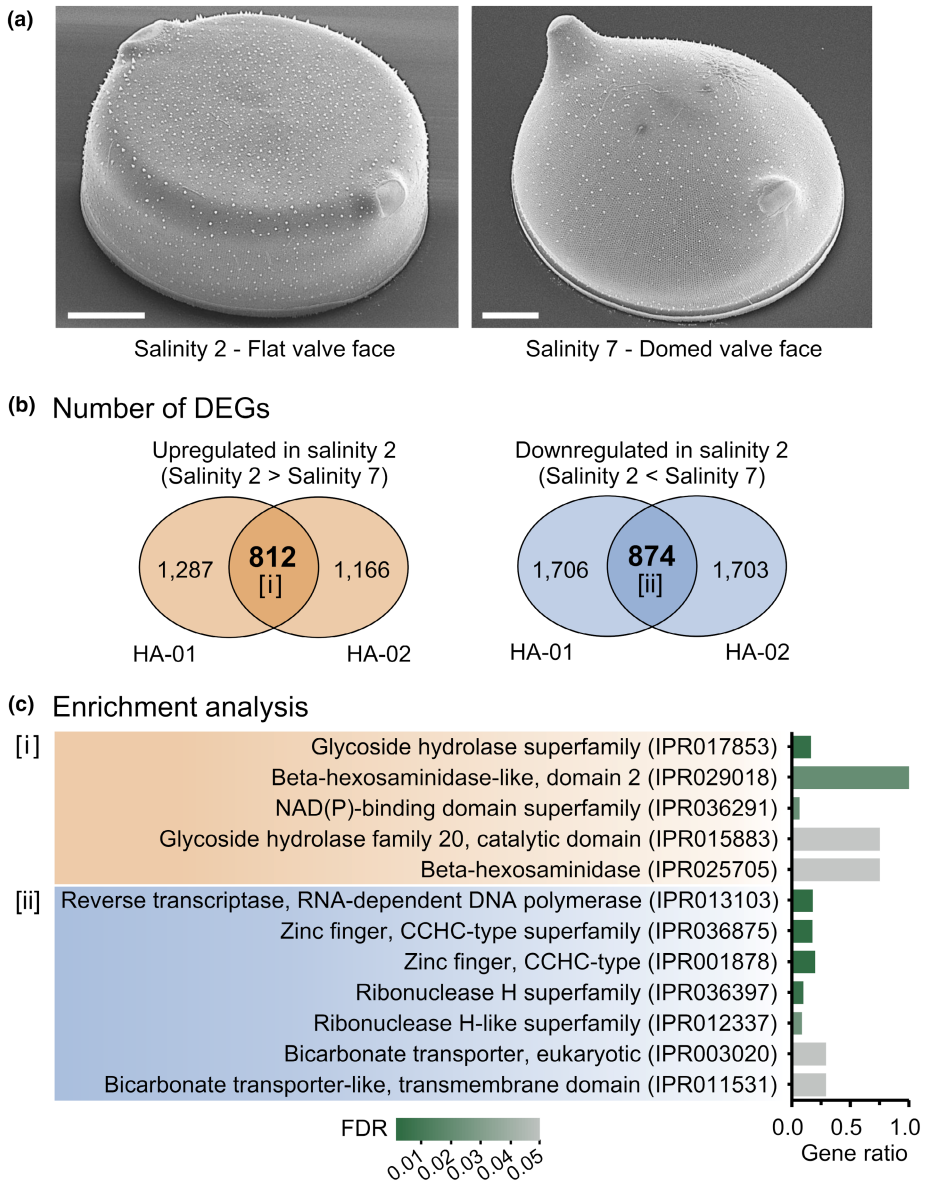

FIGURE 1 Valve morphologies of *Pleurosira laevis* triggered in salinity 2 and 7, and differentially expressed genes (DEGs) between the conditions. (a) Scanning electron microscopy pictures of the valves of *P. laevis* (HA-02) formed in salinity 2 and 7. Scale bars = 20 μm. (b) Venn diagrams showing the intersection between DEGs of the 2 strains and (c) InterPro enrichment on the shared [i] up and [ii] down-regulated genes.

we focused on this conserved response by selecting DEGs in the same direction in both strains.

Overview of the functions of shared DEGs

InterPro enrichment analysis showed NAD(P)-binding domain superfamilies (IPR017853), which are found in various enzymes, and beta-hexosaminidase (IPR029018 and IPR025705) and glycoside hydrolase families (IPR017853 and IPR015883) involved in hydrolysis of glycans were enriched in the genes up-regulated strains in salinity 2 (Figure 1c). Alternatively, in the genes down-regulated in salinity 2, the reverse transcriptase (IPR013103), ribonuclease H superfamily (IPR036397, IPR012337), and zinc finger CCHC-type (IPR036875 and IPR001878) were enriched, which are all domains related to TEs (Figure 1c). All genes assigned to zinc finger CCHC-type from the shared down-regulated genes showed hits with a reverse transcriptase of *Fragilaria crotonensis* (blastp, E-value < 6.3E-09). Furthermore, bicarbonate transporter (IPR003020 and IPR011531) was also enriched in down-regulated genes.

Transmembrane transport

A gene encoding a putative aquaporin was up-regulated in salinity 2 (TRINITY_DN11354_c0_g1, TC:1.A.8.8;

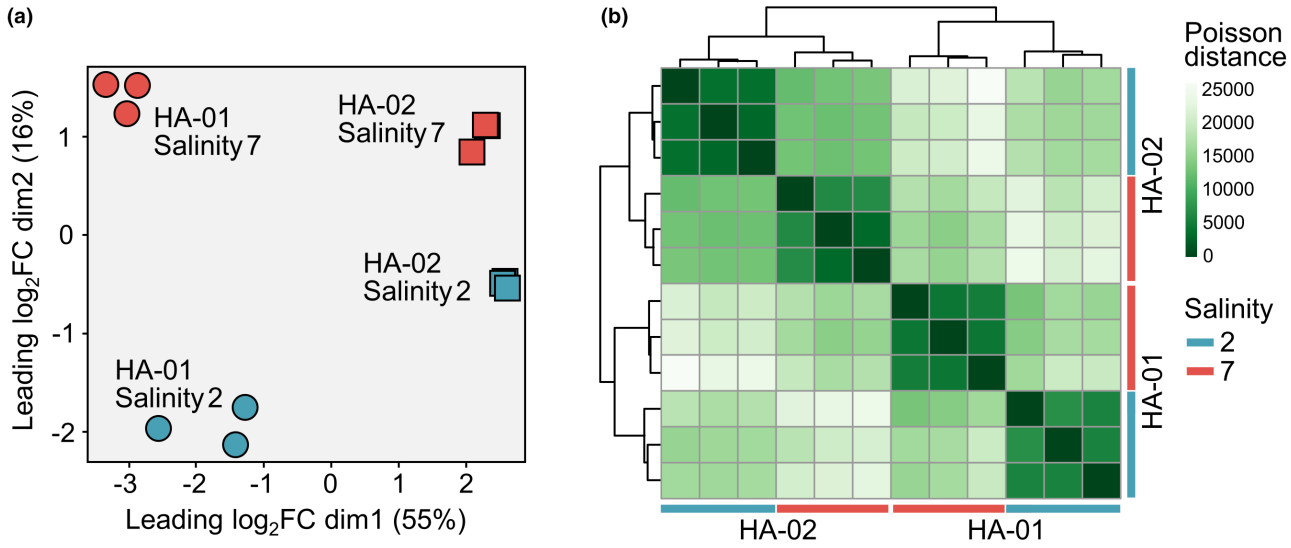

FIGURE 2 Variation among strains in the transcriptional response of *Pleurosira laevis* to salinity 2 and 7. (a) Multidimensional scaling (MDS) plot of RNA-sequencing samples. The distances between the samples were based on the Log_2 fold changes in the 500 most variable genes between the samples. (b) Poisson-distance heatmap of the full data set.

Figure 3; Table S2 in the Supporting Information). Aquaporins transport water and nonpolar molecules into or out of the cell, contributing to osmoregulation and potentially playing a role in osmotic sensing (Hill et al., 2004; Matsui et al., 2018; Tyerman et al., 2002). Our results were consistent with previous findings of up-regulated aquaporins in *Cyclotella cryptica* and *Skeletonema marinoi* under low salinity conditions (Downey et al., 2023; Pinseel et al., 2022). The betaine/carnitine/choline transporters and the proline/betaine transporters, which Nakov et al. (2020) identified as differentially expressed in the long-term osmotic response of *C. cryptica*, were not among our DEGs.

Osmotic sensing and regulation of cytosolic Ca^{2+} levels

Diatoms respond to environmental stimuli, including osmotic stress, through changes in calcium homeostasis (Falciatore et al., 2000). *Pleurosira laevis* is known to exhibit plastids assembling around the nucleus in response to contact stimuli and light irradiation. This response has been suggested to be essential for Ca^{2+} influx into the cytosol through channels (Makita & Shihira-Ishikawa, 1997; Shihira-Ishikawa et al., 2007). The genes up-regulated in salinity 2 included a putative calcium permeable stress-gated cation channel (CSC) 1-like transporter (TRINITY_DN919_c0_g2, TC:1.A.17.3). Calcium permeable stress-gated cation channels are conserved in eukaryotes and are gated by stress signals such as hyperosmotic shock, thus potentially serving as sensors linking stress stimuli to calcium-dependent downstream responses (Hou et al., 2014). Moreover, we observed mechanosensitive (MS) ion channels among the up-regulated transporters (Figure 4a). These channels are transmembrane proteins that directly link mechanical stimuli to ion fluxes and are responsible for sensing and responding to changes in membrane tension (Basu & Haswell, 2017). Two genes (TRINITY_DN7153_c0_g1 and TRINITY_DN2800_c0_g2) were putative MscS-like channels (TC:1.A.23.4), and MscS-like channels are directly gated by membrane tension and typically function to prevent cell rupture during hypoosmotic shock (Basu & Haswell, 2017). The differential expression of these CSC and MS ion channels between the conditions of salinity 2 and 7 suggests that *P. laevis* may be capable of sensing the difference in osmotic pressure and plasma membrane tension caused by such a relatively small difference in salinity. Although Downey et al. (2023) reported the activation of MS ion channels in *Cyclotella cryptica* within 3 h of hypoosmotic exposure, there are no reports showing long-term (ca. 1 month) up-regulation, as observed in *P. laevis*. In *Phaeodactylum tricornutum*, Ca^{2+} signaling induced by elevated cytosolic Ca^{2+} levels following hypoosmotic shock is important in cell volume regulation, and this elevation of cytosolic Ca^{2+} is possibly due to Ca^{2+} influx caused by increased cell volume activating MS ion channels (Helliwell et al., 2021). In our previous study (Kamakura et al., 2022), we demonstrated that morphological plasticity in the valve of this diatom was induced by osmotic changes resulting from the addition of sorbitol to the medium, and we discussed how this phenomenon could depend on plasma membrane tension at the cleavage furrow of daughter protoplasts, providing valve molding surfaces. Therefore, it is tempting to assume that Ca^{2+} signaling, brought about by the gating of MS ion channels, affects the downstream

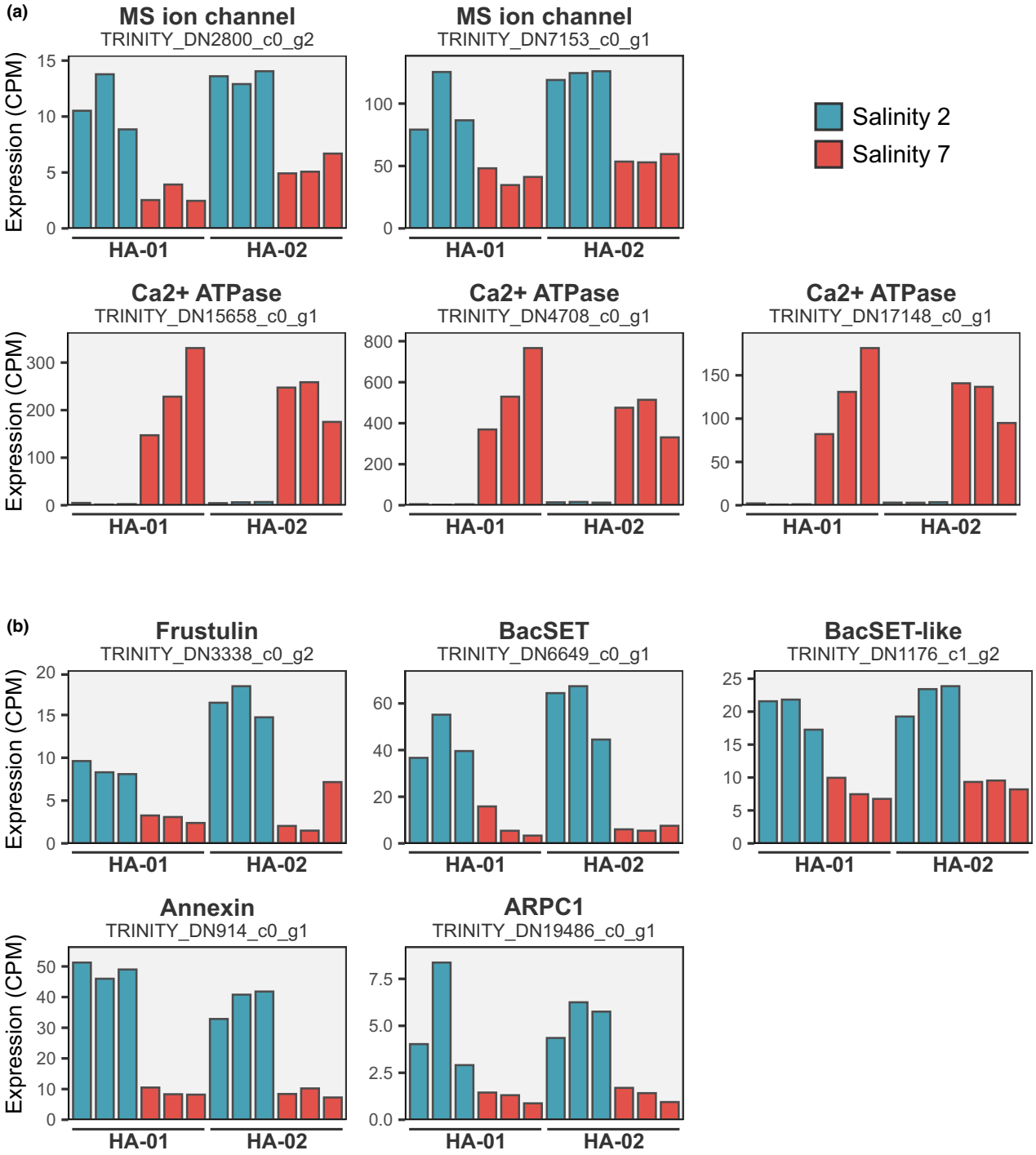

FIGURE 3 Barplots showing gene expression in salinity 2 and salinity 7 for selected Ca^{2+} transporters (a) and putative cell wall-related proteins (b). Each sample of the two strains included in this study (HA-01, HA-02) is represented by a single bar; height indicates the expression in counts per million (CPM) in that sample.

expression of genes involved in morphogenesis or cell volume regulation, ultimately resulting in changes in valve morphology.

The three P-type ATPases, which were the most down-regulated in salinity 2 (i.e., up-regulated in salinity 7, Figure 4a), were putative Ca^{2+}-ATPases (TC:3.A.3.2.29) based on the TCDB annotation (TRINITY_DN4708_c0_g1, TRINITY_DN17148_c0_g1, and TRINITY_DN15658_c0_g1). Despite the small difference in salinity, their expression levels were distinct: They were barely expressed in salinity 2 but exhibited 30–134 times higher expression in salinity 7 compared with salinity 2. Ca^{2+} ATPases are typically located in the plasma membrane or endoplasmic reticulum membrane, where they pump cytosolic Ca^{2+} out to the extracellular or

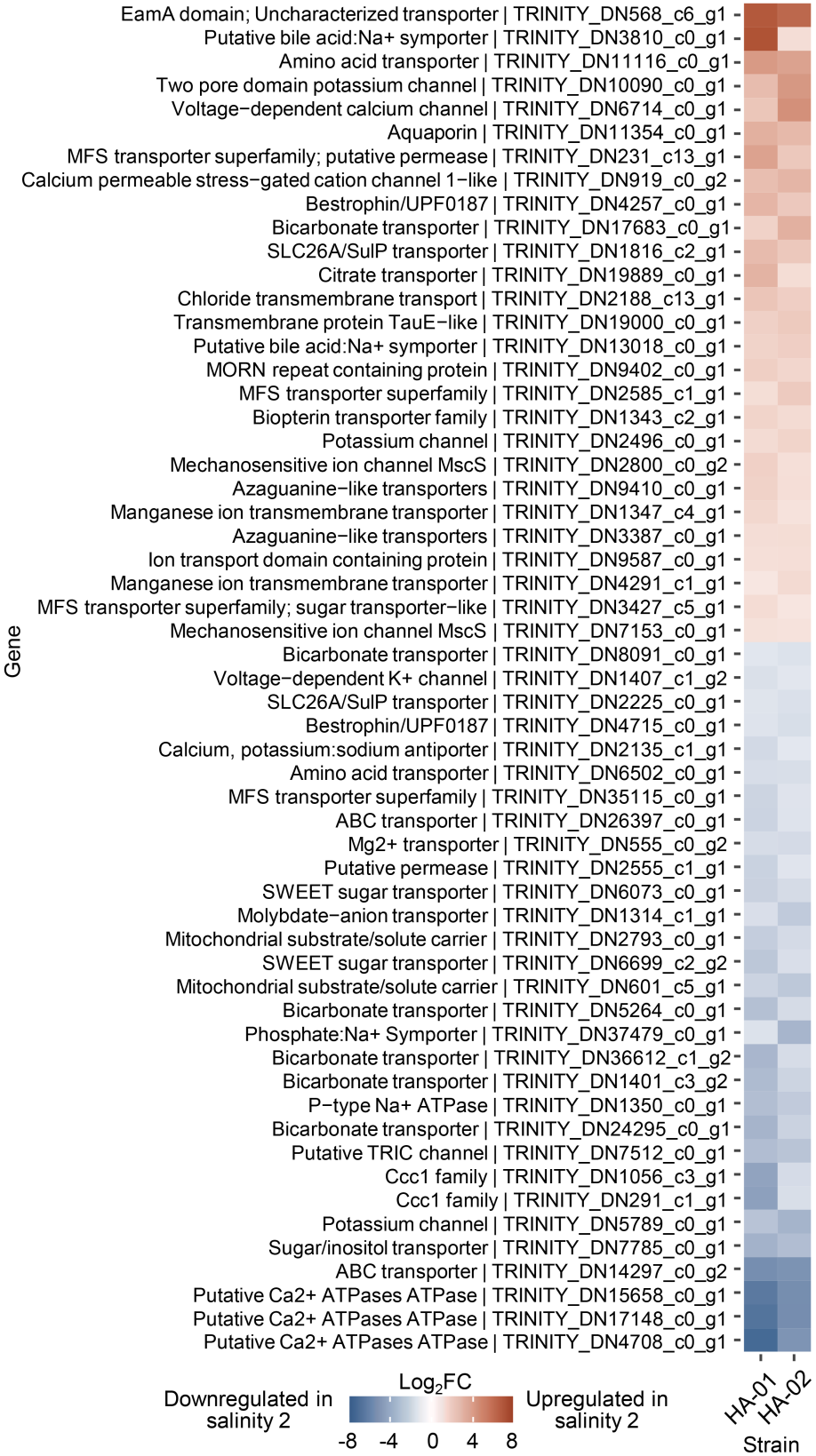

FIGURE 4 Log2 fold changes of shared differentially expressed genes (DEGs) encoding transporters.

endoplasmic reticulum space, thereby reducing cytosolic Ca^{2+} concentration to basal levels (Brini & Carafoli, 2011). Our results suggest that *Pleurosira laevis* actively exports Ca^{2+} from the cytosol in salinity 7. Although we observed an up-regulation of Ca^{2+} influx into the cytosol in response to salinity 2

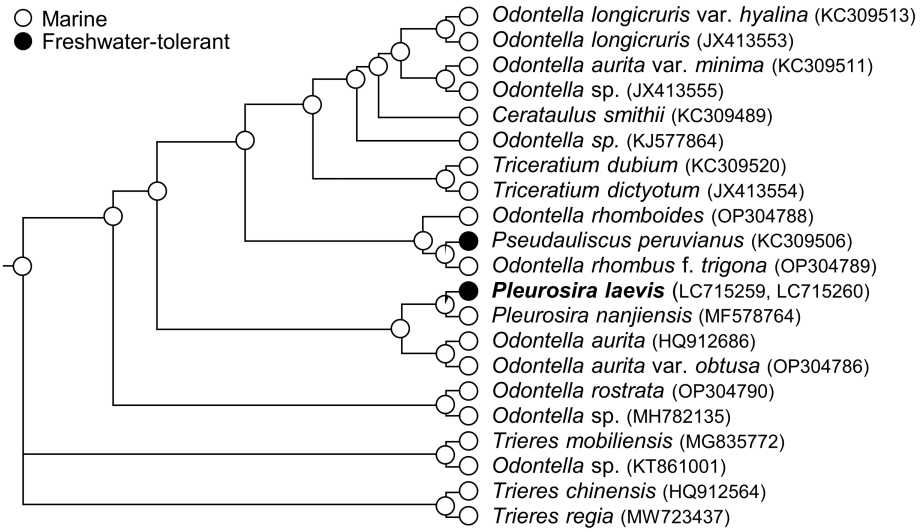

FIGURE 5 Maximum likelihood ancestral state reconstructions based on SSU rDNA gene sequences. Pie graphs at internal nodes indicate the relative maximum likelihood support for the inferred ancestral habitat type. Brackets indicate GenBank accessions. *Pseudauliscus peruvianus* was described from the Hudson River by Schmidt (1875) and was observed in the marine environment in Ashworth et al. (2013); therefore, it was assumed here to be tolerant of freshwater environment.

through MS ion channels (as discussed in the previous section), the down-regulation of Ca^{2+} efflux implies that *P. laevis* was directed toward maintaining higher cytosolic Ca^{2+} levels in salinity 2 compared with salinity 7. These Ca^{2+}-ATPases, specific to a salinity of 7, clustered together in a clade of diatom Ca^{2+}-ATPases that includes both centric and pennate sequences (Figure S3 in the Supporting Information). The closest outgroup to this clade consisted of the *Chlamydomonas reinhardtii* sequences Cre09.g410050 and Cre09.g410100, both of which were annotated as ATP2C Ca^{2+}-ATPases.

Sugar transport

We found the transporters called SWEETs within the down-regulated genes (TRINITY_DN6699_c2_g2 and TRINITY_DN6073_c0_g1, TC:2.A.123.1). Discovered in 2010 (Chen et al., 2010), SWEET is a relatively recent class of sugar transporters. These transporters are responsible for the flux of sugar molecules across membranes and are known to be involved in various physiological processes in plants, including responses to environmental stress (Breia et al., 2021; Gautam et al., 2022). Diatom genomes contain SWEET homologs (Jia et al., 2017). However, to our knowledge, there is no information available on the function and expression of these transporters in diatoms. Since sugars act as compatible solutes (Suescún-Bolívar & Thomé, 2015), the activation of SWEETs in salinity 7 might be explained by the uptake of extracellular sugars in response to higher osmotic pressures, potentially contributing to osmotic regulation.

Bicarbonate transport

Five bicarbonate transporters (HCO_3^- transporters) were down-regulated in salinity 2 (up-regulated in salinity 7, TRINITY_DN24295_c0_g1, TRINITY_DN1401_c3_g2, TRINITY_DN36612_c1_g2, TRINITY_DN5264_c0_g1, and TRINITY_DN8091_c0_g1, TC:2.A.31.1 or 2). Meanwhile, one putative bicarbonate transporter (TRINITY_DN17683_c0_g1) was up-regulated in salinity 2; however, enrichment analysis based on InterPro accessions indicated a significant enrichment of bicarbonate transporters among the down-regulated genes (Figure 1c). Some HCO_3^- transporters have been investigated in *Phaedactylum. tricornutum*. Nakajima et al. (2013) and Nawaly et al. (2023) observed that the solute carrier (SLC) 4-1 and -2 of *Ph. tricornutum* took up HCO_3^- from seawater in a Na^+-dependent manner and suggested that it was an effective CO_2 concentrating mechanism for marine diatoms to overcome CO_2 limitation in alkaline, high-salinity water. In contrast, SLC4-4 of *Ph. tricornutum* exhibits broad selectivity for cations, depending on Na^+, K^+, and Li^+ (Nawaly et al., 2023). The SLC4 homologs were suggested to be generally present in marine diatoms, both the pennates and the centrics (Nakajima et al., 2013). They have likely been derived from the ancestral eukaryotic host cell of secondary endosymbiosis, supported by their similarities to members of the mammalian SLC family (Nakajima et al., 2013). The putative HCO_3^- transporters of *Pleurosira laevis* may also be Na^+- and cation-dependent, similar to those in *Ph. tricornutum*, although they are phylogenetically distinct from these SLC4 transporters (Figure S4 in the Supporting Information). The finding

that *P. laevis* regulates HCO_3^- transport in response to salinity may explain the results of culture experiments (Kamakura et al., 2022) and the field observations (Bąk et al., 2020; Kociolek et al., 1983; Wujek & Welling, 1981) that this diatom grows well in saline environments. Other *Pleurosira* species have been collected from freshwater (*P. socotrensis*, *P. socotrensis* var. *pangeroni*, and *P. indica*), brackish (*P. socotrensis* var. *bengalensis*), and marine environments (*P. nanjiensis*), with *P. socotrensis* successfully growing in seawater medium (Compère, 1982; Karthick & Kociolek, 2011; Li et al., 2018; Li & Chiang, 1979). Additionally, *Odontella*, the genus most closely related to *Pleurosira*, consists of marine species. A phylogeny-based ancestral habitat reconstruction suggests that the ancestor of *P. laevis* was likely marine (Figure 5), and the HCO_3^- transporters were derived from the last common ancestor of the *Pleurosira* clade. It is reasonable to assume that the euryhalinity of *P. laevis* reflects the evolutionary transition in *Pleurosira* from marine to freshwater-tolerant. The active bicarbonate transport in saline environments is still conserved in *P. laevis* although this diatom is much more prevalent in brackish and freshwater environments than in full seawater.

Candidate genes involved in cell wall morphogenesis

We detected four genes encoding cell wall-related proteins that may be involved in the morphogenesis of the flat valve face, as they were up-regulated in a salinity of 2 (Figure 3b). Among these, two were BacSET proteins (TRINITY_DN6649_c0_g1 and TRINITY_DN1176_c1_g2). The BacSET protein family is a recently identified family of methyltransferases that is up-regulated during diatom morphogenesis and potentially targets long chain polyamine (LCPA) and proteins related to silica formation as substrates (Nemoto et al., 2020). The gene TRINITY_DN1176_c1_g2 is related to BacSET, but the SET domain is missing, so we refer to it as BacSET-like. Furthermore, a frustulin gene was up-regulated in salinity 2 (TRINITY_DN3338_c0_g2). Frustulins were among the first proteins to be isolated from frustules and reside in the organic casing around the silica cell wall (Kröger et al., 1996). It has been suggested that frustulins may not play a role in silica formation within the SDV (van de Poll et al., 1999). It is unclear how they affect the final valve morphology of *Pleurosira laevis*. Notably, no cell wall-related genes were detected with higher expression in a salinity of 7, so it appears that specific cell wall proteins are restricted to the formation of the flat valve morphology (salinity 2).

As the cytoskeletal elements play a crucial role in cell wall morphogenesis by interacting with the SDV (Pickett-Heaps et al., 1990; Tesson & Hildebrand, 2010a, 2010b), we turned our attention to cytoskeleton-related genes. A gene encoding Arp2/3 complex subunit 1 (ARPC1) was up-regulated in salinity 2 (TRINITY_DN19486_c0_g1). The ARPC1 gene has been shown to play a role in absorbing osmotic shock in the model organism *Physcomitrella patens* and controlling morphogenesis in the cell apex through the regulation of actin dynamics (Harries et al., 2005). These functions have been presumed to occur by influencing the Arp2/3 complex, which serves as a nucleation site for the formation of new actin filaments. Notably, the Arp2/3 complex has been presumed to be absent in diatoms (Aumeier et al., 2015). Indeed, BLASTp searches with the *Pleurosira laevis* ARPC1 protein did not reveal any homologs in the proteome of other diatom species in the NCBI and PLAZA Diatoms 1.0 databases. To our knowledge, it has not been revealed whether this subunit exhibits any special function apart from the Arp2/3 complex. We also observed that a gene encoding putative annexin was up-regulated in salinity 2 (TRINITY_DN914_c0_g1, Table S1). Annexins, which are known to be involved in various cellular functions, have been shown to be involved in Ca^{2+} influx through the plasma membrane (Demidchik et al., 2018). Additionally, annexins link Ca^{2+} signaling and actin dynamics at membrane contact sites by binding to membrane phospholipids in a Ca^{2+}-dependent manner, thus organizing the relationship between the membrane and cytoskeleton (Hayes et al., 2004). They play a role in plasma membrane repair through actin cytoskeleton remodeling triggered by Ca^{2+} influx upon membrane injury (Koerdt et al., 2019). The activation of annexin in salinity 2 in *P. laevis* may be due to an increase in cytosolic Ca^{2+} concentration as a result of channel gating by osmotic gradient and membrane tension. Although the involvement of annexin in diatom morphogenesis is not known and needs further investigation, including cellular localization analysis, it is interesting to speculate that annexin may be involved in controlling the morphology of SDV or the daughter plasma membrane to determine the resulting valve morphology on a micrometer scale. It has been speculated that the formation of the flat valve face is facilitated by the pushing of swelling daughter cells against each other at the cleavage furrow (i.e., the molding surface of new valves) in a hypoosmotic environment (Mann, 1984). In addition to this morphological control from outside the cell, our results suggest that cellular processes actively contribute to the formation of a flat valve face.

Finally, we detected DEGs of unknown function that contain ankyrin repeats (Table S3 in the Supporting Information). This domain mediates protein–protein interactions and is involved in many cellular functions (Mosavi et al., 2004). It has been suggested that ankyrin repeat-bearing proteins might play a general role in silica biosynthesis in diatoms (Bilcke et al., 2021; Heintze et al., 2022).

Although the growth rate of *Pleurosira laevis* did not differ between salinity treatments of 2 and 7 in a previous study (Kamakura et al., 2022), random differences in growth or cell cycle phasing after more than a month could be the cause of the differential expression of cell wall-related genes that we observed. To rule out this potential confounding factor, we investigated the response of a curated set of 39 marker genes for different stages of the mitotic cell cycle (G1/S, S, and M-phase) in our transcriptomic data set. Although some S- and M-phase markers were up-regulated in a salinity of 2, the majority of markers were not significantly differential expressed, did not show a consistent response between strains, or were even down-regulated (Figure S5 in the Supporting Information). Hence, it is unlikely that the strong up-regulation of cell wall genes we observed is due to an enrichment of cells in the mitosis/cytokinesis phase of the cell cycle.

Intracellular transport

We observed several DEGs related to membrane trafficking and motor protein activity (Table S4 in the Supporting Information). Silica deposition vesicles are believed to be generated by fusion of vesicles, possibly of Golgi origin (Pickett-Heaps et al., 1990; Schmid & Schulz, 1979); thus, membrane trafficking is required for frustule morphogenesis inside SDVs. Heintze et al. (2022) picked clathrin coat proteins, Arf, Rab, and v-SNARE as candidates for proteins involved in vesicular transport required for SDV biogenesis in *Thalassiosira pseudonana* through proteomic analysis of SDVs. In addition, motor proteins such as dynein and myosin are also expected to play a potential role in diatom morphogenesis due to their ability to bind to the cytoskeleton and their involvement in vesicular transport (Shrestha et al., 2012; Tanaka et al., 2015).

Transposable elements

Putative transposable elements (TEs) were abundant among DEGs, particularly among those that were down-regulated in salinity 2 (Table S5 in the Supporting Information). This result is further supported by the enrichment of TE-related InterPro accessions among the genes down-regulated in salinity 2 (Figure 1c). Transposable elements were also abundant in DEGs that were not shared between strains (Table S6 in the Supporting Information). The TEs identified in *Pleurosira laevis* were observed to include both retrotransposons that move within the genome via a "copy-and-paste" mechanism and putative DNA transposons that move via a "cut-and-paste" mechanism. The differentially expressed retrotransposons were distributed across the CoDi1-7 clades (Figure S6 in the Supporting Information). The putative DNA transposons were annotated as PiggyBac, Transposase IS4, and Tigger TE-derived protein (Tables S5 and S6). Transposable elements are known to become active under environmental changes or stress conditions (Casacuberta & González, 2013). In diatoms, up-regulation of TEs has been reported in response to thermal stress (Egue et al., 2015), high biomass density (Oliver et al., 2010), and elevated pCO_2 (Huang et al., 2019) in *Phaeodactylum tricornutum*, elevated pH in *Fragilaria crotonensis* (Zepernick et al., 2022), presence of grazers in *Skeletonema marinoi* (Amato et al., 2018), and cold stress in *Leptocylindrus aporus* (Pargana et al., 2019). In Pinseel et al. (2022), a lower salinity condition triggered the down-regulation of TEs in *S. marinoi*. Transposable elements can induce a wide range of mutations, ranging from subtle regulatory mutations to major genomic rearrangements. Because of their ability to generate the mutations and their responsiveness and sensitivity to environmental change, they have been thought to play a relevant role in adaptation (Casacuberta & González, 2013). Transponsable elements might have contributed to the genetic diversity that enables diatoms to successfully adapt to various environments (Maumus et al., 2009), although there is no evidence for a specific role for diatoms in environmental adaptation to date. In addition to the fact that TE insertions themselves can affect gene structure and expression as regulatory sequences, there are also known cases where the effects of epigenetic regulation targeting TEs extend to their neighboring genes (Lisch, 2013). Further exploration of genes located in the vicinity of TEs in the *P. laevis* genome will help us understand the genes affected by TEs and their potential association with environmental responses, including the plasticity of valve morphology.

Pleurosira laevis is regarded as an invasive species in the Great Lakes in the United States and in Europe (Hulme et al., 2009; Litchman, 2010; Olenin et al., 2017). This diatom was first described from the Hudson River, New York, US (Bailey, 1842; Ehrenberg, 1843) and has been observed in Natal, Brazil (Roper, 1859) and along the "shores of North and South America" according to Pritchard et al. (1861). However, its distribution has been expanded, as documented by more recent reports of first appearances in various regions (e.g., Lake Michigan, US: Wujek & Welling, 1981; Czech Republic: Fránková-Kozáková et al., 2007; China: Guo-Feng et al., 2008; Korea: Kim et al., 2008; Uzbekistan: Mamanazarova & Gololobova, 2017). Transposable elements may facilitate the successful invasion of alien species by promoting rapid adaptation to the environment (Stapley et al., 2015). In some invasive plants and animals, genomic evolution resulting from a TE burst has been suggested to potentially facilitate adaptation (Liu et al., 2018; Su et al., 2021). The activation of TEs in

P. laevis in response to slight salinity differences between salinity 2 and 7 might be related to the invasive aspect of this species.

Stress-responsive gene expression

The gene encoding Glutathione peroxidase (EC:1.11.1.9), involved in the degradation of reactive oxygen species (ROS), was down-regulated in salinity 2. Two genes encoding thioredoxin were up-regulated, and five were down-regulated in salinity 2 (Figure S7a in the Supporting Information). Within the xanthophyll cycle, which is known to alleviate oxidative stress in addition to its function in photosynthesis (Latowski et al., 2011), violaxanthin de-epoxidase (EC:1.23.5.1) was up-regulated in salinity 2, whereas zeaxanthin epoxidase (EC:1.14.15.21) was down-regulated in salinity 2. Genes encoding superoxide dismutase (EC:1.15.1.1) and peroxiredoxin (EC:1.11.1.24), involved in ROS removal, were not included in the DEGs shared between the strains.

Chaperones are activated to counteract protein aggregation and misfolding brought about by oxidative stress (Reichmann et al., 2018). In addition, heat shock proteins induced under stress conditions have been shown to have chaperone functions (Hendrick & Hartl, 1993). More genes encoding chaperones, heat shock proteins, and heat shock factors were down-regulated than up-regulated (Figure S7b). Although we did not see significant differences in growth rates and apparent cellular stress in *Pleurosira laevis* between salinity 2 and 7 in culture experiments (Kamakura et al., 2022), the cells appear to be sensitive to the variations in stress levels between the conditions.

Osmolyte biosynthesis

Aquatic organisms are capable of adapting to different salinities, which represent varying osmotic conditions, by maintaining osmotic balance between the external environment and their cells through transmembrane transport and the synthesis of osmolytes, also known as compatible solutes (Suescún-Bolívar & Thomé, 2015). The organic osmolytes of diatoms are, for example, free proline and other amino acids (Dickson & Kirst, 1987; Krell et al., 2007, 2008; Liu & Hellebust, 1976a, 1976b; Scholz & Liebezeit, 2012), taurine (Jackson et al., 1992), dimethylsulfoniopropionate (DMSP, Kageyama, Tanaka, Shibata, et al., 2018; Kettles et al., 2014; Lavoie et al., 2018; Lyon et al., 2011; Scholz & Liebezeit, 2012), and glycine betaine (Dickson & Kirst, 1987; Kageyama, Tanaka, & Takabe, 2018; Scholz & Liebezeit, 2012).

Two genes encoding pyrroline-5-carboxylate reductase (EC:1.5.1.2, TRINITY_DN8746_c0_g1) and proline iminopeptidase (EC:3.4.11.5, TRINITY_DN71618_c0_g1), which are involved in proline biosynthesis, were up-regulated in salinity 2. The former enzyme catalyzes the final step in proline synthesis, and its expression was up-regulated in *Fragilariopsis cylindrus* under high-salinity conditions (Krell et al., 2007). Given the importance of osmolytes, it is intriguing that our results indicate an up-regulation of proline biosynthesis at lower salinity (salinity 2) compared to salinity 7. This raises questions about the universality of proline utilization in diatoms. It should be noted that Nakov et al. (2020) and Pinseel et al. (2022) examined transcriptional responses to different salinities after long-term acclimation (120 days and >11 days, respectively) and observed that genes involved in proline biosynthesis did not consistently respond across strains to salinity. Therefore, proline may not be crucial in the long-term osmoregulation in diatoms, although it plays a role in the acute response in *Cyclotella cryprica* (Downey et al., 2023). Our observation of up-regulation in proline biosynthesis under long-term acclimation (>1 month) might be considered as falling within the range of intraspecific variation in transcriptional responses among strains if more strains were studied. No DEGs were detected for the biosynthesis of osmolytes taurine, DMSP, glycine betaine, and ectoine. We provide a section describing the details of these results on osmolyte biosynthesis and a section on metabolic pathways in Appendix S3 in the Supporting Information. Table S7 and Figures S8 and S9 in the Supporting Information are referenced within these supplementary sections.

CONCLUSIONS

Our aim was to investigate genes involved in the regulation of diatom morphology using *Pleurosira laevis*, in which a slight change in salinity had been known to induce three-dimensional morphological plasticity. Since the difference in our salinity contrast (salinity 2 vs. salinity 7) was not large, we expected to detect a smaller number of DEGs involved in osmoregulation than, for example, when comparing the response to freshwater (salinity 0) versus seawater (salinity >30). Nevertheless, it should be noted that the transcriptomic response associated with the morphological responses described here cannot be completely disentangled from those caused by osmotic changes.

Our results suggested that in a salinity of 2, which produced a flat valve face, cytosolic Ca^{2+} levels were increased due to the up-regulation of genes encoding MS ion channels and down-regulation of genes encoding Ca^{2+}-ATPases. The change in valve morphology after a salinity change has been thought to be dependent on changes in membrane tension (Schmid, 1987). In that respect, it is noteworthy that we detected an up-regulation of MS ion channels,

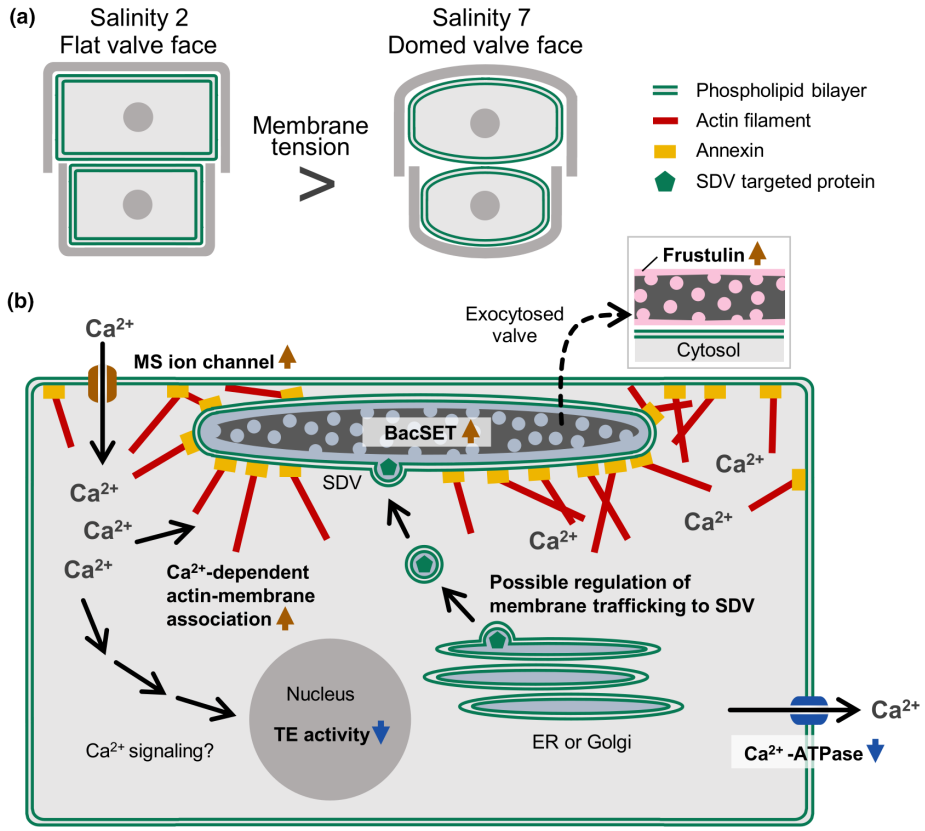

FIGURE 6 Valve morphogenesis of *Pleurosira laevis* in response to osmotic pressure and membrane tension (a) Differences in membrane tension that *P. laevis* cells experience in forming flat or domed valves. (b) Schematic diagram of the regulation of cellular functions that are possibly involved in the formation of a flat valve (salinity 2). Bolded brown and blue arrows indicate up and down-regulation, respectively, in comparison with cells with domed valves.

which play a role in sensing cell membrane tension, in response to elevated membrane tension caused by reduced osmotic pressure (Figure 6a). Furthermore, genes encoding annexin, which mediates membrane-actin filament association in a Ca^{2+}-dependent manner, and ARPC1, known for its association with the regulation of cell morphology, were up-regulated at salinity 2 (Figure 3). We hypothesize that the morphogenesis related to osmotic pressure may be achieved through an upstream response involving osmotic pressure- and membrane tension-dependent regulation of cytosolic Ca^{2+} levels through the gating of transporters such as MS ion channels, followed by a downstream response involving Ca^{2+}-dependent regulation of actin dynamics at the SDV membrane in which the new cell wall is forming (Figure 6b). These results suggest that the morphogenesis of the flat valve is not solely achieved by the passive molding of the SDV through the pressing of swelling daughter cells against each other at the cleavage furrow. Furthermore, some proteins related to the silica frustule were up-regulated in salinity 2. It should be noted that numerous ankyrin repeat-containing and membrane-trafficking proteins of unknown function were differentially expressed, although their cellular localization or targets are yet unclear. In addition, we observed that even small differences between salinity 2 and 7 induced regulations of transporter activity, responses to oxidative stress, physiological regulation, and TE activity. Taken together, these factors would contribute to the successful acclimation and colonization of this diatom in environments with varying salinities. This study highlights the sensitivity of euryhaline diatoms to environmental salinity, the fine-grained mechanisms to cope with osmotic pressure and suggests an active role of cellular processes in controlling valve morphology under different osmotic pressures.

AUTHOR CONTRIBUTIONS

Shiho Kamakura: Conceptualization (supporting); data curation (lead); investigation (lead); methodology (lead); visualization (equal); writing – original draft (lead); writing – review and editing (equal). **Gust Bilcke:** Data curation (supporting); formal analysis (supporting); investigation (supporting); methodology (supporting); visualization (equal); writing – original draft (supporting); writing – review and editing (equal). **Shinya Sato:** Conceptualization (lead); funding acquisition (lead); project administration (lead); resources (lead); supervision (lead); writing – original draft (supporting); writing – review and editing (equal).

ACKNOWLEDGMENTS

We thank Prof. David G. Mann for his helpful comments in interpreting the results. SK received support from the Morishita-Jintan Scholarship Foundation. GB is a post-doctoral fellow supported by Fonds Wetenschappelijk Onderzoek (FWO, 1228423N). This work was financially supported by JSPS KAKENHI (grant number: 20K06726) and Grant-in-Aid for Scientific Research on Innovative Areas 21A402. NGS data analysis was performed on the NIG supercomputer at ROIS National Institute of Genetics.

ORCID

Shiho Kamakura https://orcid.org/0000-0003-0251-6900
Gust Bilcke https://orcid.org/0000-0002-9499-2295
Shinya Sato https://orcid.org/0000-0001-6649-6975

REFERENCES

Al-Shahrour, F., Minguez, P., Tárraga, J., Medina, I., Alloza, E., Montaner, D., & Dopazo, J. (2007). FatiGO +: A functional profiling tool for genomic data. Integration of functional annotation, regulatory motifs and interaction data with microarray experiments. *Nucleic Acids Research*, *35*, W91–W96. https://doi.org/10.1093/nar/gkm260

Amato, A., Sabatino, V., Nylund, G. M., Bergkvist, J., Basu, S., Andersson, X. M., Sanges, R., Godhe, A., Kiørboe, T., Selander, E., & Ferrante, I. M. (2018). Grazer-induced transcriptomic and metabolomic response of the chain-forming diatom *Skeletonema marinoi*. *The ISME Journal*, *12*(6), 1594–1604. https://doi.org/10.1038/s41396-018-0094-0

Aramaki, T., Blanc-Mathieu, R., Endo, H., Ohkubo, K., Kanehisa, M., Goto, S., & Ogata, H. (2020). KofamKOALA: KEGG ortholog assignment based on profile HMM and adaptive score threshold. *Bioinformatics*, *36*(7), 2251–2252. https://doi.org/10.1093/bioinformatics/btz859

Ashworth, M. P., Nakov, T., & Theriot, E. C. (2013). Revisiting Ross and Sims (1971): Toward a molecular phylogeny of the Biddulphiaceae and Eupodiscaceae (Bacillariophyceae). *Journal of Phycology*, *49*(6), 1207–1222. https://doi.org/10.1111/jpy.12131

Aumeier, C. (2014). The cytoskeleton of diatoms: Structural and genomic analysis. [Ph.D. dissertation, University of Bonn, Bonn].

Aumeier, C., Polinski, E., & Menzel, D. (2015). Actin, actin-related proteins and profilin in diatoms: A comparative genomic analysis. *Marine Genomics*, *23*, 133–142. https://doi.org/10.1016/j.margen.2015.07.002

Bailey, J. W. (1842). A sketch of the Infusoria of the family Bacillaria, with some account of the most interesting species which have been found in a recent or fossil state in the United States. Part II. *American Journal of Science*, *42*, 88–105.

Bąk, M., Halabowski, D., Kryk, A., Lewin, I., & Sowa, A. (2020). Mining salinisation of rivers: Its impact on diatom (Bacillariophyta) assemblages. *Fottea*, *20*(1), 1–16. https://doi.org/10.5507/fot.2019.010

Balzano, S., Sarno, D., & Kooistra, W. H. (2011). Effects of salinity on the growth rate and morphology of ten *Skeletonema* strains. *Journal of Plankton Research*, *33*(6), 937–945. https://doi.org/10.1093/plankt/fbq150

Basu, D., & Haswell, E. S. (2017). Plant mechanosensitive ion channels: An ocean of possibilities. *Current Opinion in Plant Biology*, *40*, 43–48. https://doi.org/10.1016/j.pbi.2017.07.002

Bilcke, G., Osuna-Cruz, C. M., Santana Silva, M., Poulsen, N., D'hondt, S., Bulankova, P., Vyverman, W., De Veylder, L., & Vandepoele, K. (2021). Diurnal transcript profiling of the diatom *Seminavis robusta* reveals adaptations to a benthic lifestyle. *The Plant Journal*, *107*, 315–336. https://doi.org/10.1111/tpj.15291

Breia, R., Conde, A., Badim, H., Fortes, A. M., Gerós, H., & Granell, A. (2021). Plant SWEETs: From sugar transport to plant-pathogen interaction and more unexpected physiological roles. *Plant Physiology*, *186*(2), 836–852. https://doi.org/10.1093/plphys/kiab127

Brini, M., & Carafoli, E. (2011). The plasma membrane Ca^{2+} ATPase and the plasma membrane sodium calcium exchanger cooperate in the regulation of cell calcium. *Cold Spring Harbor Perspectives in Biology*, *3*(2), a004168. https://doi.org/10.1101/cshperspect.a004168

Bucchini, F., Del Cortona, A., Kreft, Ł., Botzki, A., Van Bel, M., & Vandepoele, K. (2021). TRAPID 2.0: A web application for taxonomic and functional analysis of de novo transcriptomes. *Nucleic Acids Research*, *49*(27), e101. https://doi.org/10.1093/nar/gkab565

Capella-Gutiérrez, S., Silla-Martínez, J. M., & Gabaldón, T. (2009). trimAl: A tool for automated alignment trimming in large-scale phylogenetic analyses. *Bioinformatics*, *25*(15), 1972–1973. https://doi.org/10.1093/bioinformatics/btp348

Casacuberta, E., & González, J. (2013). The impact of transposable elements in environmental adaptation. *Molecular Ecology*, *22*(6), 1503–1517. https://doi.org/10.1111/mec.12170

Chen, L. Q., Hou, B. H., Lalonde, S., Takanaga, H., Hartung, M. L., Qu, X. Q., Guo, W. J., Kim, J. G., Underwood, W., Chaudhuri, B., Chermak, D., Antony, G., White, F. F., Shauna, S. C., Mudgett, M. B., & Frommer, W. B. (2010). Sugar transporters for intercellular exchange and nutrition of pathogens. *Nature*, *468*, 527–532. https://doi.org/10.1038/nature09606

Chen, S., Zhou, Y., Chen, Y., & Gu, J. (2018). Fastp: An ultra-fast all-in-one FASTQ preprocessor. *Bioinformatics*, *34*(17), i884–i1890. https://doi.org/10.1093/bioinformatics/bty560

Compère, P. (1982). Taxonomic revision of the diatom genus *Pleurosira* (Eupodiscaceae). *Bacillaria*, *5*, 165–190.

Conesa, A., Götz, S., García-Gómez, J. M., Terol, J., Talón, M., & Robles, M. (2005). Blast2GO: A universal tool for annotation, visualization and analysis in functional genomics research. *Bioinformatics*, *21*(18), 3674–3676. https://doi.org/10.1093/bioinformatics/bti610

De Sanctis, S., Wenzler, M., Kröger, N., Malloni, W. M., Sumper, M., Deutzmann, R., Zadravec, P., Brunner, E., Kremer, W., & Kalbitzer, H. R. (2016). PSCD domains of Pleuralin-1 from the diatom *Cylindrotheca fusiformis*: NMR structures and interactions with other biosilica-associated proteins. *Structure*, *24*(7), 1178–1191. https://doi.org/10.1016/j.str.2016.04.021

Demidchik, V., Shabala, S., Isayenkov, S., Cuin, T. A., & Pottosin, I. (2018). Calcium transport across plant membranes: Mechanisms and functions. *New Phytologist*, *220*(1), 49–69. https://doi.org/10.1111/nph.15266

Dickson, D. M. J., & Kirst, G. O. (1987). Osmotic adjustment in marine eukaryotic algae: The role of inorganic ions, quaternary ammonium, tertiary sulphonium and carbohydrate solutes. I. Diatoms and a rhodophyte. *New Phytologist*, *106*(4), 645–655.

Downey, K. M., Judy, K. J., Pinseel, E., Alverson, A. J., & Lewis, J. A. (2023). The dynamic response to hypo-osmotic stress reveals distinct stages of freshwater acclimation by a euryhaline diatom. *Molecular Ecology*, *32*(11), 2766–2783. https://doi.org/10.1111/mec.16703

Egue, F., Chenais, B., Tastard, E., Marchand, J., Hiard, S., Gateau, H., Hermann, D., Morant-Manceau, A., Casse, N., & Caruso, A. (2015). Expression of the retrotransposons *Surcouf* and *Blackbeard* in the marine diatom *Phaeodactylum tricornutum* under thermal stress. *Phycologia*, *54*(6), 617–627. https://doi.org/10.2216/15-52.1

Ehrenberg, C. G. (1843). Verbreitung und Einfluß des mikroskopischen Lebens in Süd- und Nord-Amerika [Distribution and influence of microscopic life in South and North America]. *Abhandlungen der Königlichen Akademie der Wissenschaften Zu Berlin*, *1841*, 291–466.

Emms, D. M., & Kelly, S. (2019). OrthoFinder: Phylogenetic orthology inference for comparative genomics. *Genome Biology*, *20*, 238. https://doi.org/10.1186/s13059-019-1832-y

Falciatore, A., d'Alcalà, M. R., Croot, P., & Bowler, C. (2000). Perception of environmental signals by a marine diatom. *Science*, *288*(5475), 2363–2366. https://doi.org/10.1126/science.288.5475.2363

Finkel, Z. V., & Kotrc, B. (2010). Silica use through time: Macroevolutionary change in the morphology of the diatom frustule. *Geomicrobiology Journal*, *27*(6–7), 596–608. https://doi.org/10.1080/01490451003702941

Fránková-Kozáková, M., Marvan, P., & Geriš, R. (2007). Halophilous diatoms in Czech running waters: *Pleurosira laevis* and *Bacillaria paxillifera*. In W. H. Kusber & R. Jahn (Eds.), *Proceedings of the 1st Central European Diatom Meeting. Berlin, Germany, 2007* (pp. 39–44). Boletim do Museu Botanico Municipal.

Fu, L., Niu, B., Zhu, Z., Wu, S., & Li, W. (2012). CD-HIT: Accelerated for clustering the next-generation sequencing data. *Bioinformatics*, *28*(23), 3150–3152. https://doi.org/10.1093/bioinformatics/bts565

Gautam, T., Dutta, M., Jaiswal, V., Zinta, G., Gahlaut, V., & Kumar, S. (2022). Emerging roles of SWEET sugar transporters in plant development and abiotic stress responses. *Cell*, *11*(8), 1303. https://doi.org/10.3390/cells11081303

Görlich, S., Pawolski, D., Zlotnikov, I., & Kröger, N. (2019). Control of biosilica morphology and mechanical performance by the conserved diatom gene Silicanin-1. *Communications Biology*, *2*, 1–8. https://doi.org/10.1038/s42003-019-0436-0

Götz, S., Garcia-Gomez, J. M., Terol, J., Williams, T. D., Nagaraj, S. H., Nueda, M. J., Robles, M., Talon, M., Dopazo, J., & Conesa, A. (2008). High-throughput functional annotation and data mining with the Blast2GO suite. *Nucleic Acids Research*, *36*(10), 3420–3435. https://doi.org/10.1093/nar/gkn176

Grabherr, M., Haas, B. J., Yassour, M., Levin, J. Z., Thompson, D. A., Amit, I., Adiconis, X., Fan, L., Raychowdhury, R., Zeng, Q., Chen, Z., Mauceli, E., Hacohen, N., Gnirke, A., Rhind, N., Palma, F., Birren, B. F., Nusbaum, C., Lindblad-Toh, K., … Regev, A. (2011). Full-length transcriptome assembly from RNA-seq data without a reference genome. *Nature Biotechnology*, *29*, 644–652. https://doi.org/10.1038/nbt.1883

Grigoriev, I. V., Hayes, R. D., Calhoun, S., Kamel, B., Wang, A., Ahrendt, S., Dusheyko, S., Nikitin, R., Mondo, S. J., Salamov, A., Shabalov, I., & Kuo, A. (2021). PhycoCosm, a comparative algal genomics resource. *Nucleic Acids Research*, *49*(D1), D1004–D1011. https://doi.org/10.1093/nar/gkaa898

Guillard, R. R., & Lorenzen, C. J. (1972). Yellow-green algae with chlorophyllide C 1, 2. *Journal of Phycology*, *8*(1), 10–14. https://doi.org/10.1111/j.1529-8817.1972.tb03995.x

Guo-Feng, P., Guo-Xiang, L., Zheng-Yu, H., & Guo-Xiang, L. (2008). *Pleurosira laevis* (Ehrenberg) Compère, a new record freshwater diatom from China. *Journal of Wuhan Botanical Research*, *26*(5), 458–460.

Hall, T. (1999). BioEdit: A user-friendly biological sequence alignment editor and analysis program for windows 95/98/NT. *Nucleic Acids Symposium Series*, *41*, 95–98.

Harries, P. A., Pan, A., & Quatrano, R. S. (2005). Actin-related protein 2/3 complex component ARPC1 is required for proper cell morphogenesis and polarized cell growth in *Physcomitrella patens*. *Plant Cell*, *17*(8), 2327–2739. https://doi.org/10.1105/tpc.105.033266

Hayes, M. J., Rescher, U., Gerke, V., & Moss, S. E. (2004). Annexin–actin interactions. *Traffic*, *5*(8), 571–576. https://doi.org/10.1111/j.1600-0854.2004.00210.x

Heintze, C., Babenko, I., Žáčková Suchanová, J., Skeffington, A., Friedrich, B. M., & Kröger, N. (2022). The molecular basis for pore pattern morphogenesis in diatom silica. *Proceedings of the National Academy of Sciences*, *119*(49), e2211549119. https://doi.org/10.1073/pnas.2211549119

Helliwell, K. E., Kleiner, F. H., Hardstaff, H., Chrachri, A., Gaikwad, T., Salmon, D., Smirnoff, N., Wheeler, G. L., & Brownlee, C. (2021). Spatiotemporal patterns of intracellular Ca^{2+} signalling govern hypo-osmotic stress resilience in marine diatoms. *New Phytologist*, *230*(1), 155–170. https://doi.org/10.1111/nph.17162

Hendrick, P. J., & Hartl, F. U. (1993). Molecular chaperone functions of heat-shock proteins. *Annual Review of Biochemistry*, *62*, 349–384. https://doi.org/10.1146/annurev.bi.62.070193.002025

Hill, A., Shachar-Hill, B., & Shachar-Hill, Y. (2004). What are aquaporins for? *The Journal of Membrane Biology*, *197*, 1–32. https://doi.org/10.1007/s00232-003-0639-6

Hou, C., Tian, W., Kleist, T., He, K., Garcia, V., Bai, F., Hao, Y., Luan, S., & Li, L. (2014). DUF221 proteins are a family of osmosensitive calcium-permeable cation channels conserved across eukaryotes. *Cell Research*, *24*, 632–635. https://doi.org/10.1038/cr.2014.14

Huang, R., Ding, J., Gao, K., Cruz de Carvalho, M. H., Tirichine, L., Bowler, C., & Lin, X. (2019). A potential role for epigenetic processes in the acclimation response to elevated pCO_2 in the model diatom *Phaeodactylum tricornutum*. *Frontiers in Microbiology*, *9*, 3342. https://doi.org/10.3389/fmicb.2018.03342

Hulme, P. E., Roy, D. B., Cunha, T., & Larsson, T.-B. (Eds). (2009). List of species alien in Europe and to Europe. In *Handbook of alien species in Europe, invading nature* (pp. 133–263). Springer. https://doi.org/10.1007/978-1-4020-8280-1_11

Imaizumi, T., Kanegae, T., & Wada, M. (2000). Cryptochrome nucleocytoplasmic distribution and gene expression are regulated by light quality in the fern *Adiantum capillus-veneris*. *The Plant Cell*, *12*(1), 81–95. https://doi.org/10.1105/tpc.12.1.81

Jackson, A. E., Ayer, S. W., & Laycock, M. V. (1992). The effect of salinity on growth and amino acid composition in the marine diatom *Nitzschia pungens*. *Canadian Journal of Botany*, *70*, 2198–2201. https://doi.org/10.1139/b92-272

Jia, B., Zhu, X. F., Pu, Z. J., Duan, Y. X., Hao, L. J., Zhang, J., Chen, L. Q., Jeon, C. O., & Xuan, Y. H. (2017). Integrative view of the diversity and evolution of SWEET and SemiSWEET sugar transporters. *Frontiers in Plant Science*, *8*, 2178. https://doi.org/10.3389/fpls.2017.02178

Jones, P., Binns, D., Chang, H. Y., Fraser, M., Li, W., McAnulla, C., McWilliam, H., Maslen, J., Mitchell, A., Nuka, G., Pesseat, S., Quinn, F. A., Sangrador-Vegas, A., Scheremetjew, M., Yong, S. Y., Lopez, R., & Hunter, S. (2014). InterProScan 5: Genome-scale protein function classification. *Bioinformatics*, *30*(9), 1236–1240. https://doi.org/10.1093/bioinformatics/btu031

Kageyama, H., Tanaka, Y., Shibata, A., Waditee-Sirisattha, R., & Takabe, T. (2018). Dimethylsulfoniopropionate biosynthesis in a diatom *Thalassiosira pseudonana*: Identification of a gene encoding MTHB-methyltransferase. *Archives of Biochemistry and Biophysics*, *645*(1), 100–106. https://doi.org/10.1016/j.abb.2018.03.019

Kageyama, H., Tanaka, Y., & Takabe, T. (2018). Biosynthetic pathways of glycinebetaine in *Thalassiosira pseudonana*; functional characterization of enzyme catalyzing three-step methylation of glycine. *Plant Physiology and Biochemistry*, *127*, 248–255. https://doi.org/10.1016/j.plaphy.2018.03.032

Kamakura, S., Ashworth, M. P., Yamada, K., Mikami, D., Kobayashi, A., Idei, M., & Sato, S. (2022). Morphological plasticity in response to salinity change in the euryhaline diatom *Pleurosira laevis* (Bacillariophyta). *Journal of Phycology*, *58*(5), 631–642. https://doi.org/10.1111/jpy.13277

Karthick, B., & Kociolek, J. P. (2011). Four new centric diatoms (Bacillariophyceae) from the Western Ghats, South India.

Phytotaxa, *22*, 25–40. https://doi.org/10.11646/phytotaxa.22.1.2

Katoh, K., Misawa, K., Kuma, K., & Miyata, T. (2002). MAFFT: A novel method for rapid multiple sequence alignment based on fast Fourier transform. *Nucleic Acids Research*, *30*(14), 3059–3066. https://doi.org/10.1093/nar/gkf436

Keeling, P. J., Burki, F., Wilcox, H. M., Allam, B., Allen, E. E., Amaral-Zettler, L. A., Armbrust, E. V., Archibald, J. M., Bharti, A. K., Bell, C. J., Beszteri, B., Bidle, K. D., Cameron, C. T., Campbell, L., Caron, D. A., Cattolico, R. A., Collier, J. L., Coyne, K., Davy, S. K., … Worden, A. Z. (2014). The marine microbial eukaryote transcriptome sequencing project (MMETSP): Illuminating the functional diversity of eukaryotic life in the oceans through transcriptome sequencing. *PLoS Biology*, *12*(6), e1001889. https://doi.org/10.1371/journal.pbio.1001889

Kettles, N. L., Kopriva, S., & Malin, G. (2014). Insights into the regulation of DMSP synthesis in the diatom *Thalassiosira pseudonana* through APR activity, proteomics and gene expression analyses on cells acclimating to changes in salinity, light and nitrogen. *PLoS ONE*, *9*(4), e94795. https://doi.org/10.1371/journal.pone.0094795

Khabudaev, K. V., Petrova, D. P., Bedoshvili, Y. D., Likhoshway, Y. V., & Grachev, M. A. (2022). Molecular evolution of tubulins in diatoms. *International Journal of Molecular Sciences*, *23*(2), 618. https://doi.org/10.3390/ijms23020618

Kim, Y., Suk Choi, J., Sin Kim, J., Hee Kim, S., Chan Park, J., & Won Kim, H. (2008). The effects of effluent from a closed mine and treated sewage on epilithic diatom communities in a Korean stream. *Nova Hedwigia*, *86*(3–4), 507–524. https://doi.org/10.1127/0029-5035/2008/0086-0507

Kociolek, J. P., Lamb, M. A., & Lowe, R. L. (1983). Notes on the growth and ultrastructure of *Biddulphia laevis* Ehr. (Bacillariophyceae) in the Maumee River, Ohio. *The Ohio Journal of Science*, *83*(3), 125–130.

Koerdt, S. N., Ashraf, A. P. K., & Gerke, V. (2019). Annexins and plasma membrane repair. *Current Topics in Membranes*, *84*, 43–65. https://doi.org/10.1016/bs.ctm.2019.07.006

Krell, A., Beszteri, B., Dieckmann, G., Glöckner, G., Valentin, K., & Mock, T. (2008). A new class of ice-binding proteins discovered in a salt-stress-induced cDNA library of the psychrophilic diatom *Fragilariopsis cylindrus* (Bacillariophyceae). *European Journal of Phycology*, *43*(4), 423–433. https://doi.org/10.1080/09670260802348615

Krell, A., Funck, D., Plettner, I., John, U., & Dieckmann, G. (2007). Regulation of proline metabolism under salt stress in the psychrophilic diatom *Fragilariopsis cylindrus* (Bacillariophyceae). *Journal of Phycology*, *43*(4), 753–762. https://doi.org/10.1111/j.1529-8817.2007.00366.x

Kröger, N., Bergsdorf, C., & Sumper, M. (1996). Frustulins: Domain conservation in a protein family associated with diatom cell walls. *European Journal of Biochemistry*, *239*(2), 259–264. https://doi.org/10.1111/j.1432-1033.1996.0259u.x

Kröger, N., Lorenz, S., & Brunner, E. (2002). Self-assembly of highly phosphorylated silaffins and their function in biosilica morphogenesis. *Science*, *298*(5593), 584–586. https://doi.org/10.1126/science.1076221

Kröger, N., & Poulsen, N. (2008). Diatoms—From cell wall biogenesis to nanotechnology. *Annual Review of Genetics*, *42*, 83–107. https://doi.org/10.1146/annurev.genet.41.110306.130109

Kumar, S., Stecher, G., & Tamura, K. (2016). MEGA7: Molecular evolutionary genetics analysis version 7.0 for bigger datasets. *Molecular Biology and Evolution*, *33*(7), 1870–1874. https://doi.org/10.1093/molbev/msw054

Latowski, D., Kuczyńska, P., & Strzałka, K. (2011). Xanthophyll cycle –a mechanism protecting plants against oxidative stress. *Redox Report*, *16*(2), 78–90. https://doi.org/10.1179/174329211X13020951739938

Lavoie, M., Waller, J. C., Kiene, R. P., & Levasseur, M. (2018). Polar marine diatoms likely take up a small fraction of dissolved dimethylsulfoniopropionate relative to bacteria in oligotrophic environments. *Aquatic Microbial Ecology*, *81*, 213–218. https://doi.org/10.3354/ame01871

Li, B., & Dewey, C. N. (2011). RSEM: Accurate transcript quantification from RNA-seq data with or without a reference genome. *BMC Bioinformatics*, *12*, 323. https://doi.org/10.1186/1471-2105-12-323

Li, C. W., & Chiang, Y. (1979). A euryhaline and polymorphic new diatom, *Proteucylindrus taiwanensis* gen. et sp. nov. *British Phycological Journal*, *14*, 377–384. https://doi.org/10.1080/00071617900650431

Li, Y., Nagumo, T., & Xu, K. (2018). Morphology and molecular phylogeny of *Pleurosira nanjiensis* sp. nov., a new marine benthic diatom from the Nanji Islands, China. *Acta Oceanologica Sinica*, *37*, 33–39. https://doi.org/10.1007/s13131-018-1298-x

Lisch, D. (2013). How important are transposons for plant evolution? *Nature Reviews Genetics*, *14*, 49–61. https://doi.org/10.1038/nrg3374

Litchman, E. (2010). Invisible invaders: Non-pathogenic invasive microbes in aquatic and terrestrial ecosystems. *Ecology Letters*, *13*(12), 1560–1572. https://doi.org/10.1111/j.1461-0248.2010.01544.x

Liu, C., Zhang, Y., Ren, Y., Wang, H., Li, S., Jiang, F., Yin, L., Qiao, X., Zhang, G., Qian, W., Liu, B., & Fan, W. (2018). The genome of the golden apple snail *Pomacea canaliculata* provides insight into stress tolerance and invasive adaptation. *GigaScience*, *7*(9), giy101. https://doi.org/10.1093/gigascience/giy101

Liu, M. S., & Hellebust, J. A. (1976a). Effects of salinity and osmolarity of the medium on amino acid metabolism in *Cyclotella cryptica*. *Canadian Journal of Botany*, *54*(9), 938–948. https://doi.org/10.1139/b76-098

Liu, M. S., & Hellebust, J. A. (1976b). Regulation of proline metabolism in the marine centric diatom *Cyclotella cryptica*. *Canadian Journal of Botany*, *54*(9), 949–959. https://doi.org/10.1139/b76-099

Llorens, C., Futami, R., Covelli, L., Dominguez-Escriba, L., Viu, J. M., Tamarit, D., Aguilar-Rodriguez, J., Vicente-Ripolles, M., Fuster, G., Bernet, G. P., Maumus, F., Munoz-Pomer, A., Sempere, J. M., LaTorre, A., & Moya, A. (2011). The gypsy database (GyDB) of mobile genetic elements: Release 2.0. *Nucleic Acids Research*, *39*(Database issue), D70–D74. https://doi.org/10.1093/nar/gkq1061

Lyon, B. R., Lee, P. A., Bennett, J. M., DiTullio, G. R., & Janech, M. G. (2011). Proteomic analysis of a sea-ice diatom: Salinity acclimation provides new insight into the dimethylsulfoniopropionate production pathway. *Plant Physiology*, *157*(4), 1926–1941. https://doi.org/10.1104/pp.111.185025

Maddison, W. P., & Maddison, D. R. (2021). Mesquite: A modular system for evolutionary analysis. Version 3.70. http://www.mesquiteproject.org

Makita, N., & Shihira-Ishikawa, I. (1997). Chloroplast assemblage by mechanical stimulation and its intercellular transmission in diatom cells. *Protoplasma*, *197*, 86–95. https://doi.org/10.1007/BF01279887

Mamanazarova, K. S., & Gololobova, M. A. (2017). First record of diatom species *Pleurosira laevis* (Ehrenberg) Compère for Uzbekistan and Central Asia. *Russian Journal of Biological Invasions*, *8*, 69–74. https://doi.org/10.1134/S2075111717010088

Mann, D. G. (1984). An ontogenetic approach to diatom systematics. In D. G. Mann (Ed.), *Proceedings of the 7th international diatom symposium, Philadelphia, 1982* (pp. 113–144). Koeltz.

Mann, D. G. (1999). Crossing the Rubicon: The effectiveness of the marine/freshwater interface as a barrier to the migration of diatom germplasm. In S. Mayama, M. Idei, & I. Koizumi (Eds.),

Proceedings of the 14th international diatom symposium, Tokyo, 1996 (pp. 1–21). Koeltz.

Matsui, H., Hopkinson, B. M., Nakajima, K., & Matsuda, Y. (2018). Plasma membrane-type aquaporins from marine diatoms function as CO_2/NH_3 channels and provide photoprotection. *Plant Physiology*, *178*(1), 345–357. https://doi.org/10.1104/pp.18.00453

Maumus, F., Allen, A. E., Mhiri, C., Hu, H., Jabbari, K., Vardi, A., Grandbastien, M. A., & Bowler, C. (2009). Potential impact of stress activated retrotransposons on genome evolution in a marine diatom. *BMC Genomics*, *10*, 624. https://doi.org/10.1186/1471-2164-10-624

Menzel, P., Ng, K. L., & Krogh, A. (2016). Fast and sensitive taxonomic classification for metagenomics with kaiju. *Nature Communications*, *7*, 1–9. https://doi.org/10.1038/ncomms11257

Mistry, J., Chuguransky, S., Williams, L., Qureshi, M., Salazar, G. A., Sonnhammer, E. L. L., Tosatto, S. C. E., Paladin, L., Raj, S., Richardson, L. J., Finn, R. D., & Bateman, A. (2021). Pfam: The protein families database in 2021. *Nucleic Acids Research*, *49*(D1), D412–D419. https://doi.org/10.1093/nar/gkaa913

Mosavi, L. K., Cammett, T. J., Desrosiers, D. C., & Peng, Z. Y. (2004). The ankyrin repeat as molecular architecture for protein recognition. *Protein Science*, *13*(6), 1435–1448. https://doi.org/10.1110/ps.03554604

Nakajima, K., Tanaka, A., & Matsuda, Y. (2013). SLC4 family transporters in a marine diatom directly pump bicarbonate from seawater. *Proceedings of the National Academy of Sciences*, *110*(5), 1767–1772. https://doi.org/10.1073/pnas.1216234110

Nakov, T., Judy, K. J., Downey, K. M., Ruck, E. C., & Alverson, A. J. (2020). Transcriptional response of osmolyte synthetic pathways and membrane transporters in a euryhaline diatom during long-term acclimation to a salinity gradient. *Journal of Phycology*, *56*(6), 1712–1728. https://doi.org/10.1111/jpy.13061

Nawaly, H., Matsui, H., Tsuji, Y., Iwayama, K., Ohashi, H., Nakajima, K., & Matsuda, Y. (2023). Multiple plasma membrane SLC4s contribute to external HCO_3^- acquisition during CO_2 starvation in the marine diatom *Phaeodactylum tricornutum*. *Journal of Experimental Botany*, *74*(1), 296–307. https://doi.org/10.1093/jxb/erac380

Nemoto, M., Iwaki, S., Moriya, H., Monden, Y., Tamura, T., Inagaki, K., Mayama, S., & Obuse, K. (2020). Comparative gene analysis focused on silica cell wall formation: Identification of diatom-specific SET domain protein methyltransferases. *Marine Biotechnology*, *22*, 551–563. https://doi.org/10.1007/s10126-020-09976-1

Nguyen, L. T., Schmidt, H. A., von Haeseler, A., & Minh, B. Q. (2015). IQ-TREE: A fast and effective stochastic algorithm for estimating maximum-likelihood phylogenies. *Molecular Biology and Evolution*, *32*(1), 268–274. https://doi.org/10.1093/molbev/msu300

Olenin, S., Gollasch, S., Lehtiniemi, M., Sapota, M., & Zaiko, A. (2017). Biological invasions. In P. Snoeijs-Leijonmalm, H. Schubert, & T. Radziejewska (Eds.), *Biological oceanography of the Baltic Sea* (p. 193–232). Springer. https://doi.org/10.1007/978-94-007-0668-2_5

Oliver, M. J., Schofield, O., & Bidle, K. (2010). Density dependent expression of a diatom retrotransposon. *Marine Genomics*, *3*(3–4), 145–150. https://doi.org/10.1016/j.margen.2010.08.006

Osuna-Cruz, C. M., Bilcke, G., Vancaester, E., de Decker, S., Bones, A. M., Winge, P., Poulsen, N., Bulankova, P., Verhelst, B., Audoor, S., Belisova, D., Pargana, A., Russo, M., Stock, F., Cirri, E., Brembu, T., Pohnert, G., Piganeau, G., Ferrante, M. I., … Vandepoele, K. (2020). The *Seminavis robusta* genome provides insights into the evolutionary adaptations of benthic diatoms. *Nature Communications*, *11*, 3320. https://doi.org/10.1038/s41467-020-17191-8

Paasche, E., Johansson, S., & Evensen, D. L. (1975). An effect of osmotic pressure on the valve morphology of the diatom *Skeletonema subsalsum* (a. Cleve) Bethge. *Phycologia*, *14*(4), 205–211. https://doi.org/10.2216/i0031-8884-14-4-205.1

Pargana, A., Musacchia, F., Sanges, R., Russo, M. T., Ferrante, M. I., Bowler, C., & Zingone, A. (2019). Intraspecific diversity in the cold stress response of transposable elements in the diatom *Leptocylindrus aporus*. *Genes*, *11*(1), 9. https://doi.org/10.3390/genes11010009

Paysan-Lafosse, T., Blum, M., Chuguransky, S., Grego, T., Pinto, B. L., Salazar, A. G., Bileschi, L. M., Bork, P., Bridge, A., Colwell, L., Gough, J., Haft, H. D., Letunić, I., Marchler-Bauer, A., Mi, H., Natale, A. D., Orengo, A. C., Pandurangan, P. A., Rivoire, C., … Bateman, A. (2023). InterPro in 2022. *Nucleic Acids Research*, *51*(D1), D418–D427. https://doi.org/10.1093/nar/gkac993

Pickett-Heaps, J., Schmid, A. M. M., & Edgar, L. A. (1990). The cell biology of diatom valve formation. In F. E. Round & D. J. Chapman (Eds.), *Progress in phycological research* (Vol. 7, pp. 1–168). Biopress.

Pinseel, E., Nakov, T., Van den Berge, K., Downey, K. M., Judy, K. J., Kourtchenko, O., Kremp, A., Ruck, E. C., Sjöqvist, C., Töpel, M., Godhe, A., & Alverson, A. J. (2022). Strain-specific transcriptional responses overshadow salinity effects in a marine diatom sampled along the Baltic Sea salinity cline. *The ISME Journal*, *16*, 1776–1787. https://doi.org/10.1038/s41396-022-01230-x

Pritchard, A., Arlidge, J. T., Archer, W., Rafts, J., & Williamson, W. C. (1861). *A history of infusoria, including the Desmidiaceae and Diatomaceae, British and foreign* (4th ed.). Whittaker and Co.

Reichmann, D., Voth, W., & Jakob, U. (2018). Maintaining a healthy proteome during oxidative stress. *Molecular Cell*, *69*(2), 203–213. https://doi.org/10.1016/j.molcel.2017.12.021

Ritchie, M. E., Phipson, B., Wu, D., Hu, Y., Law, C. W., Shi, W., & Smyth, G. K. (2015). Limma powers differential expression analyses for RNA-sequencing and microarray studies. *Nucleic Acids Research*, *43*(7), e47. https://doi.org/10.1093/nar/gkv007

Robinson, M. D., McCarthy, D. J., & Smyth, G. K. (2010). edgeR: A Bioconductor package for differential expression analysis of digital gene expression data. *Bioinformatics*, *26*(1), 139–140. https://doi.org/10.1093/bioinformatics/btp616

Robinson, M. D., & Oshlack, A. (2010). A scaling normalization method for differential expression analysis of RNA-seq data. *Genome Biology*, *11*, R25. https://doi.org/10.1186/gb-2010-11-3-r25

Roper, F. C. S. (1859). On the genus *Biddulphia* and its affinities. *Transactions of the Microscopical Society of London*, *7*, 1–24.

Saier, M. H., Reddy, V. S., Moreno-Hagelsieb, G., Hendargo, K. J., Zhang, Y., Iddamsetty, V., Lam, K. J. K., Tian, N., Russum, S., Wang, J., & Medrano-Soto, A. (2021). The transporter classification database (TCDB): 2021 update. *Nucleic Acids Research*, *49*(D1), D461–D467. https://doi.org/10.1093/nar/gkaa1004

Scheffel, A., Poulsen, N., Shian, S., & Kröger, N. (2011). Nanopatterned protein microrings from a diatom that direct silica morphogenesis. *Proceedings of the National Academy of Sciences*, *108*(8), 3175–3180. https://doi.org/10.1073/pnas.1012842108

Schmid, A. M. M. (1987). Morphogenetic forces in diatom cell wall formation. In J. Bereiter-Hahn, O. R. Anderson, & W. E. Reif (Eds.), *Cytomechanics* (pp. 183–199). Springer. https://doi.org/10.1007/978-3-642-72863-1_12

Schmid, A. M. M., & Schulz, D. (1979). Wall morphogenesis in diatoms: Deposition of silica by cytoplasmic vesicles. *Protoplasma*, *100*, 267–288. https://doi.org/10.1007/BF01279316

Schmidt, A. (1875). *Atlas der Diatomaceen-kunde [Atlas of Diatomology]. Series I: Heft 8* (pp. 29–32). Verlag von Ernst Schlegel.

Scholz, B., & Liebezeit, G. (2012). Compatible solutes in three marine intertidal microphytobenthic Wadden Sea diatoms exposed to different salinities. *European Journal of Phycology*, *47*(4), 393–407. https://doi.org/10.1080/09670262.2012.720714

Shen, W., Le, S., Li, Y., & Hu, F. (2016). SeqKit: A cross-platform and ultrafast toolkit for FASTA/Q file manipulation. *PLoS ONE*, *11*(10), e0163962. https://doi.org/10.1371/journal.pone.0163962

Shihira-Ishikawa, I., Nakamura, T., Higashi, S. I., & Watanabe, M. (2007). Distinct responses of chloroplasts to blue and green laser microbeam irradiations in the centric diatom *Pleurosira laevis*. *Photochemistry and Photobiology*, *83*(5), 1101–1109. https://doi.org/10.1111/j.1751-1097.2007.00167.x

Shrestha, R. P., Tesson, B., Norden-Krichmar, T., Federowicz, S., Hildebrand, M., & Allen, A. E. (2012). Whole transcriptome analysis of the silicon response of the diatom *Thalassiosira pseudonana*. *BMC Genomics*, *13*, 499. https://doi.org/10.1186/1471-2164-13-499

Stamatakis, A. (2014). RAxML version 8: A tool for phylogenetic analysis and post-analysis of large phylogenies. *Bioinformatics*, *30*(9), 1312–1313. https://doi.org/10.1093/bioinformatics/btu033

Stapley, J., Santure, A. W., & Dennis, S. R. (2015). Transposable elements as agents of rapid adaptation may explain the genetic paradox of invasive species. *Molecular Ecology*, *24*(9), 2241–2252. https://doi.org/10.1111/mec.13089

Su, Y., Huang, Q., Wang, Z., & Wang, T. (2021). High genetic and epigenetic variation of transposable elements: Potential drivers to rapid adaptive evolution for the noxious invasive weed *Mikania micrantha*. *Ecology and Evolution*, *11*(19), 13501–13517. https://doi.org/10.1002/ece3.8075

Suescún-Bolívar, L. P., & Thomé, P. E. (2015). Osmosensing and osmoregulation in unicellular eukaryotes. *World Journal of Microbiology and Biotechnology*, *31*, 435–443. https://doi.org/10.1007/s11274-015-1811-8

Tanaka, A., De Martino, A., Amato, A., Montsant, A., Mathieu, B., Rostaing, P., Tirichine, L., & Bowler, C. (2015). Ultrastructure and membrane traffic during cell division in the marine pennate diatom *Phaeodactylum tricornutum*. *Protist*, *166*(5), 506–521. https://doi.org/10.1016/j.protis.2015.07.005

Tesson, B., & Hildebrand, M. (2010a). Extensive and intimate association of the cytoskeleton with forming silica in diatoms: Control over patterning on the meso- and micro-scale. *PLoS ONE*, *5*(12), e14300. https://doi.org/10.1371/journal.pone.0014300

Tesson, B., & Hildebrand, M. (2010b). Dynamics of silica cell wall morphogenesis in the diatom *Cyclotella cryptica*: Substructure formation and the role of microfilaments. *Journal of Structural Biology*, *169*(1), 62–74. https://doi.org/10.1016/j.jsb.2009.08.013

Tesson, B., Lerch, S. J. L., & Hildebrand, M. (2017). Characterization of a new protein family associated with the silica deposition vesicle membrane enables genetic manipulation of diatom silica. *Scientific Reports*, *7*, 1–13. https://doi.org/10.1038/s41598-017-13613-8

Thompson, J. D., Higgins, D. G., & Gibson, T. J. (1994). CLUSTAL W: Improving the sensitivity of progressive multiple sequence alignment through sequence weighting, position-specific gap penalties and weight matrix choice. *Nucleic Acids Research*, *22*(22), 4673–4680. https://doi.org/10.1093/nar/22.22.4673

Trofimov, A. A., Pawlicki, A. A., Borodinov, N., Mandal, S., Mathews, T. J., Hildebrand, M., Ziatdinov, M. A., Hausladen, K. A., Urbanowicz, P. K., Steed, C. A., Ievlev, A. V., Belianinov, A., Michener, J. K., Vasudevan, R., & Ovchinnikova, O. S. (2019). Deep data analytics for genetic engineering of diatoms linking genotype to phenotype via machine learning. *npj Computational Materials*, *5*, 1–8. https://doi.org/10.1038/s41524-019-0202-3

Tyerman, S. D., Niemietz, C. M., & Bramley, H. (2002). Plant aquaporins: Multifunctional water and solute channels with expanding roles. *Plant, Cell & Environment*, *25*(2), 173–194. https://doi.org/10.1046/j.0016-8025.2001.00791.x

van de Poll, W. H., Vrieling, E. G., & Gieskes, W. W. C. (1999). Location and expression of frustulins in the pennate diatoms *Cylindrotheca fusiformis*, *Navicula pelliculosa*, and *Navicula salinarum* (Bacillariophyceae). *Journal of Phycology*, *35*(5), 1044–1053. https://doi.org/10.1046/j.1529-8817.1999.3551044.x

Witten, D. M. (2011). Classification and clustering of sequencing data using a Poisson model. *Annals of Applied Statistics*, *5*(4), 2493–2518. https://doi.org/10.1214/11-AOAS493

Wujek, D. E., & Welling, M. L. (1981). The occurrence of 2 centric diatoms new to the Great Lakes, USA. *Journal of Great Lakes Research*, *7*(1), 55–56. https://doi.org/10.1016/S0380-1330(81)72024-0

Zepernick, B. N., Niknejad, D. J., Stark, G. F., Truchon, A. R., Martin, R. M., Rossignol, K. L., Paerl, H. W., & Wilhelm, S. W. (2022). Morphological, physiological, and transcriptional responses of the freshwater diatom *Fragilaria crotonensis* to elevated pH conditions. *Frontiers in Microbiology*, *13*, 1044464. https://doi.org/10.3389/fmicb.2022.1044464

Zhang, Z., Schwartz, S., Wagner, L., & Miller, W. (2000). A greedy algorithm for aligning DNA sequences. *Journal of Computational Biology*, *7*(1–2), 203–214. https://doi.org/10.1089/10665270050081478

SUPPORTING INFORMATION

Additional supporting information can be found online in the Supporting Information section at the end of this article.

Data S1.

How to cite this article: Kamakura, S., Bilcke, G., & Sato, S. (2024). Transcriptional responses to salinity-induced changes in cell wall morphology of the euryhaline diatom *Pleurosira laevis*. *Journal of Phycology*, *00*, 1–19. https://doi.org/10.1111/jpy.13437